eNeuro

Research Article: New Research | Neuronal Excitability

A Neuronal activity-Dependent Dual Function chromatin-Modifying Complex Regulates *Arc* Expression

PHF8-TIP60 Regulates Arc Transcription

Nicodemus E. Oey[1], How Wing Leung[1], Rajaram Ezhilarasan[1], Lei Zhou[2], Roger W. Beuerman[2], Hendrika M.A. VanDongen[1] and Antonius M.J. VanDongen[1]

[1]*Program in Neuroscience and Behavioral Disorders, Duke-NUS Graduate Medical School, Singapore, 169857, Singapore*

[2]*Singapore Eye Research Institute, Singapore*

DOI: 10.1523/ENEURO.0020-14.2015

Received: 13 September 2014

Revised: 18 January 2015

Accepted: 22 January 2015

Published: 27 January 2015

Author contributions: N.E.O. and A.M.V. designed research; N.E.O., H.W.L., R.E., L.Z., H.V., and A.M.V. performed research; N.E.O., H.W.L., R.E., L.Z., R.W.B., H.V., and A.M.V. analyzed data; N.E.O., H.W.L., L.Z., R.W.B., H.V., and A.M.V. wrote the paper; R.E., L.Z., R.W.B., H.V., and A.M.V. contributed unpublished reagents/analytic tools.

Funding: Ministry of Education, Singapore
MOE2012-T2-1-039

Conflict of Interest: Authors report no conflict of interest

This work was supported by grant MOE2012-T2-1-039 from the Singapore Ministry of Education to A.M.J.V.D. and an award from the Singapore Ministry of Health and A*STAR, the Agency for Science, Technology and Research

Corresponding Author: Antonius M.J. VanDongen, Tel. (+65) 90606457, Email antonius.vandongen@duke-nus.edu.sg).

Cite as: eNeuro 2015; 10.1523/ENEURO.0020-14.2015

eNeuro

http://eneuro.msubmit.net

eN-NWR-0020-14R2

A neuronal activity-dependent dual function chromatin-modifying complex regulates Arc expression

1. Manuscript Title:

A neuronal activity-dependent dual function chromatin-modifying complex regulates *Arc* expression

2. Abbreviated Title:

Epigenetic regulation of Arc transcription

3. Names and Affiliations:

Nicodemus E. Oey[1*], How Wing Leung[1], Rajaram Ezhilarasan[1], Lei Zhou[2], Roger W. Beuerman[2], Hendrika M.A. VanDongen[1] and Antonius M.J. VanDongen[1]

1. Program in Neuroscience and Behavioral Disorders, Duke-NUS Graduate Medical School, Singapore 169857, Singapore
2. Singapore Eye Research Institute, Singapore

4. Author contributions

NEO Performed Research, Analyzed Data and Wrote Paper
LHW Performed Research, Analyzed Data and Wrote Paper
LZ Performed Research, Analyzed Data and Wrote Paper
RWB Performed Research, Analyzed Data
HMAVD Performed Research, Analyzed Data
AMJVD Designed Experiments, Analyzed data, Wrote Paper

5. Corresponding Author:

Antonius M.J. VanDongen
Email antonius.vandongen@duke-nus.edu.sg
Tel. (+65) 6516-7075

6. Number of figures: 10

7. Number of Tables: 0

8. Number of Multimedia: 0

9. Number of words for Abstract: 248

10. Number of words for Significance Statement: 121

11. Number of words for Introduction: 550

12. Number of words for Discussion: 2434

13. Acknowledgements: The super-resolution imaging (3D-STORM) was done with the help of the Nikon Imaging Centre (NIC) at the Singapore Bioimaging Consortium (SBIC). We would like to thank Petra de Graaf for the human FLAG-PHF8 construct which was used for sequence validation. We would like to acknowledge the help of members of the Patrick Casey laboratory, including Ms. Udhaya Kumari, for expertise in biochemistry, as well as the members of the Antonius VanDongen laboratory, including Gokulakrishna Banumurthy, Knvul Sheikh, and Dr. Ju Han.

14. Conflict of Interest: A. Authors report no conflict of interest

15. Funding sources: This work was supported by grant MOE2012-T2-1-039 from the Singapore Ministry of Education to A.M.J.V.D. and an award from the Singapore Ministry of Health and A*STAR, the Agency for Science, Technology and Research

A neuronal activity-dependent dual function chromatin-modifying complex regulates *Arc* expression

Abstract

Chromatin modification is an important epigenetic mechanism underlying neuroplasticity. Histone methylation and acetylation have both been shown to modulate gene expression, but the machinery responsible for mediating these changes in neurons has remained elusive. Here we identify a chromatin-modifying complex containing the histone demethylase PHF8 and the acetyltransferase TIP60 as a key regulator of the activity-induced expression of Arc, an important mediator of synaptic plasticity. Clinically, mutations in PHF8 cause X-linked mental retardation while TIP60 has been implicated in the pathogenesis of Alzheimer's disease. Within minutes of increased synaptic activity, this dual function complex is rapidly recruited to the Arc promoter where it specifically counteracts the transcriptionally repressive histone mark H3K9me2 to facilitate the formation of the transcriptionally permissive H3K9acS10P, thereby favoring transcriptional activation. Consequently, gain-of-function of the PHF8-TIP60 complex in primary rat hippocampal neurons has a positive effect on early activity-induced *Arc* gene expression, whereas interfering with the function of this complex abrogates it. A global proteomics screen revealed that the majority of common interactors of PHF8 and TIP60 were involved in mRNA processing, including PSF, an important molecule involved in neuronal gene regulation. Finally, we proceeded to show using super-resolution microscopy that PHF8 and TIP60 interact at the single molecule level with PSF, thereby situating this chromatin modifying complex at the crossroads of transcriptional activation. These findings point toward a mechanism by which an epigenetic pathway can regulate neuronal activity-dependent gene transcription, which has implications in the development of novel therapeutics for disorders of learning and memory.

Significance Statement

The regulation of neuronal gene expression requires dynamic changes in chromatin structure as evidenced by the fact that dysregulation of the enzymes responsible for chromatin modification often leads to intellectual disability. In this article we characterize a chromatin-modifying complex containing the X-linked mental retardation-associated protein

PHF8 and the Alzheimer's disease-associated protein TIP60 which regulates the expression of an important neuronal activity-dependent gene, *Arc*. By interfering with the enzymatic function of this complex, we show that it is possible to alter the ability of neurons to induce transcription in response to synaptic activity. This work supports an enzymatic mechanism for the epigenetic control of neuronal transcriptional programs with implications in the possible development of novel therapeutics for disorders of learning and memory.

Introduction

Activity-dependent transcription of effector genes, a pre-requisite for memory formation (Tzingounis and Nicoll, 2006), is a highly complex process (Inoue et al., 2010, West and Greenberg, 2011). Several epigenetic mechanisms have been put forth to explain the remarkable ability of neurons to dynamically regulate gene expression, including chromatin modification, which is capable of altering gene expression programs and even induce alternative splicing (Day and Sweatt, 2011). The importance of chromatin modification in learning and memory is demonstrated by the fact that dysfunction of chromatin-modifying enzymes causes severe memory impairment, which ranges from Alzheimer's disease to intellectual disability (Lewis et al., 1981, Lubin et al., 2011, Ronan et al., 2013). Recent evidence has shown that the rapid induction of immediate-early genes (IEGs) such as *Arc,* in response to neuronal activity is mediated by a mechanism involving the escape of promoter-proximal RNA Polymerase II into transcriptional elongation (Kim et al., 2010, Saha et al., 2011). The idea that stimulus-dependent rapid gene induction is controlled at the level of transcriptional elongation and mRNA processing is conserved across many cell types and is likely to be mediated by modification to chromatin structure (Hargreaves et al., 2009). Both the acetylation and methylation of histones have been purported to be important in activity-dependent gene transcription (Gupta-Agarwal et al., 2014, Lopez-Atalaya and Barco, 2014, Sen, 2014). Nevertheless, although it is known that enzymes are likely responsible for the chromatin modifications that contribute to neuronal gene activation, the nature of these epigenetic regulators is still obscure.

Here we report that the histone demethylase PHF8 cooperates with the acetyltransferase TIP60 in an activity-dependent manner to enable the rapid induction of the immediate-early gene *Arc* by specifically regulating H3K9acS10P, a dual-chromatin mark that is required for transcriptional activation. As no direct interaction between a demethylase and an

acetyltransferase has yet been reported, we focused on precisely characterizing the localization of PHF8 and TIP60 using multi-colour super-resolution microscopy and investigated their physical interaction using co-immunoprecipitation and proximity in-situ ligation. Within minutes of neural network activation, we found that the complex containing PHF8 and TIP60 specifically upregulated the transcriptional-elongation associated mark H3K9acS10P, which is required for rapid gene induction through a mechanism that likely involves transcriptional elongation. Upon verifying that this complex is able to regulate the methylation and acetylation of transcriptionally active H3K4me3-positive histones, we examined the PHF8-TIP60 interactome through immunoprecipitation followed by mass spectrometry, which revealed that the majority of PHF8 and TIP60 interacting partners are indeed involved in transcription and RNA processing. Overexpression of PHF8, but not the inactive mutant PHF8-F279S (Koivisto et al., 2007), increased neuronal H3K9acS10P and *Arc* expression, whereas RNAi-mediated knockdown of PHF8 inhibited both activity-induced H3K9acS10P and *Arc.* Furthermore, both PHF8 and TIP60 were found to be recruited to the *Arc* promoter within minutes of neuronal activation. Finally, using single-molecule imaging techniques, we demonstrate that the two chromatin-modifying enzymes have a well-defined 3-dimentional spatial relationship with each other, with each molecule occupying long-stranded structures which are closely associated with their common binding partner, PTB-associated Splicing Factor (PSF), at the nucleosomal scale. The direct interaction between the chromatin modifier PHF8 with PSF, a long term memory-associated splicing factor (Antunes-Martins et al., 2007, Kim et al., 2011) lends further evidence to the role of chromatin modification in transcriptional activation and co-transcriptional splicing in neuronal activity-dependent gene regulation.

Methods

Constructs and cloning

Full-length PHF8 was cloned through reverse transcriptase reaction of human brain cDNA (Marathon), and confirmed via Sanger sequencing against a construct of FLAG-PHF8 which was a generous gift from Petra de Graaf (Fortschegger et al., 2010). Fusion fluorescent constructs PHF8-mTurquoise2, PHF8-YFP, PHF8-tdTomato, were cloned by inserting the full-length PHF8 PCR product flanked by SalI and AgeI sites in-frame into the multiple cloning sites of the respective vectors. To generate PHF8-FLAG and TIP60-FLAG, the YFP sequence was excised with NotI and an oligonucleotide encoding the FLAG peptide sequence was annealed and ligated to the C-terminus of PHF8 and TIP60. Mutagenesis of PHF8 into PHF8-F279S was performed using the megaprimer method(Bloomer et al., 2007) by first performing a PCR with a reverse primer containing the single nucleotide mutation (c.836C>T) to generate a forward primer for a second PCR reaction amplifying the full-length gene.

Neuronal Cell Culture

Hippocampi and cortices from E18 Sprague-Dawley rats of either sex were dissected aseptically, digested using a papain dissociation system (Worthington Biochemical Corporation), and cultured in media supplemented with B27 (Brewer and Price, 1996). The appropriate density of neurons were plated on poly-D-lysine-coated glass-bottom culture dishes (MatTek, Ashland, MA), 8-well Lab-Tek II chambered cover-glass (Nunc, Denmark), or 96-well glass-bottom plates (Nunc, Denmark) that had been double-coated with poly-D-lysine overnight. Neurons were fed weekly by replacing half of the medium. HEK293, HeLa, and U2OS cells were obtained from the author's University Cell Culture Facility, and were cultured in high glucose DMEM (Gibco) with 10% fetal bovine serum (Invitrogen Corporation, Carlsbad, CA) and 1% Penicillin-Streptomycin. Cells were plated on the poly-D-lysine coated glass-bottom dishes for imaging or the Lab-Tek II chambered cover-glasses for super-resolution imaging.

Transfections and Neuronal Stimulations

Primary neurons were transfected between DIV 12 and 21 as previously described, with a few modifications (Van de Ven et al., 2005). Briefly, Lipofectamine:DNA complexes were formed in a suitable amount of Neuronal Transfection Media (BrainBits, UK) for 15 minutes at room temperature (RT). Neuronal growth medium was aspirated and the complexes were added to the neurons for 15 minutes, after which the neuronal medium was restored. HEK293, U2OS, and HeLa cells were transfected similarly, except that DMEM with high glucose media was used and the Lipofectamine 2000/ DNA mixture was added directly to existing media. Each well in a six-well plate was transfected with a 2:1 ratio of transfection reagent to plasmid DNA. To stimulate synaptic NMDA receptors and network activity (Hardingham et al., 2001), a combination of 4-Aminopyridine (4AP), Bicuculline (Bic), and Forskolin at a final

concentration of 100μM, 50μM, and 50 μM respectively were added to the medium for the appropriate amount of time. In control wells, the same volume of vehicle (DMSO) was added to neurons before lysates were collected.

Immunofluorescence

For construct co-expression experiments, transfected neuron/HEK293 cells were fixed with a solution containing 4% paraformaldehyde (PFA), 4% sucrose, and 1× PBS for 15 min at 4 °C. The cells were subsequently incubated with 1μM DAPI for 10 minutes, and preserved in 97% Thiodiethanol (TDE, Sigma). For immunostaining, cells were fixed with 100% MeOH at -20°C for 10 min. Neurons/HEK293 cells were blocked with a solution containing 10% goat or donkey serum, 2% bovine serum albumin (BSA), and 1× PBS for 1 hour at room temperature (RT), except when the goat-anti-TIP60 (K-17, Santa Cruz) antibody was used, in which case blocking was done with 10% Horse Serum in PBS-0.1% Triton X. The primary antibodies were incubated for 1 hour at RT in a dilution buffer containing 1:1 block solution and PBS-Triton X solution at the following dilutions: Mouse-anti-Arc (C7) 1:300 (Santa Cruz), Goat-anti-TIP60 (K17) 1:300, Rabbit-anti-TIP60 1:300 (Novus Biologicals), Rabbit-anti-H3K9acS10P 1:300 (Abcam). Dishes were washed 5 x 10 minutes with PBS-Triton X and incubated with Alexa-Fluor488, Alexa-Fluor568, or Alexa-Fluor647 conjugated secondary antibodies (Molecular Probes-Invitrogen) 1:1000 in dilution buffer for 1 hour at RT. Washing was repeated as per the above for 5 x 10 min and dishes were then stained with 1 μM DAPI for 10 minutes to label DNA, followed by mounting in 10%, 25%, 50%, and finally 97% Thiodiethanol (TDE).

Proximity Ligation In-Situ Assay

Stably transfected HEK293 cells expressing PHF8-YFP were fixed with 4% PFA for 15 min at 4 °C, and blocked and permeabilized using a solution containing 10% donkey serum and 0.5% Tween-20 at 37 °C. Cells were incubated overnight with primary antibodies: Mouse-anti-GFP (1:1000, Roche) and Goat-anti-TIP60 (1:300, Santa Cruz) were used to detect PHF8 and TIP60, respectively. Cells were washed five times with Buffer A (10 mM Tris, 150 mM NaCl, and 0.05% Tween-20), and then incubated for 2 hours with secondary antibodies conjugated to PLA probes: Duolink II anti-Mouse plus and Duolink II anti-Goat minus were diluted in antibody diluent to a concentration of 1:5 (OLink Bioscience) at 37 °C. After five more washes with buffer A at room temperature, hybridization was performed by incubating at 37 °C with the ligation solution (Duolink II Ligase, 1:40) for exactly 30 minutes. Ligation was stopped by a wash step and detection of the amplified probe was done with the Duolink II Detection Reagents Kit (Red). After a final wash step of 15 minutes x 5 in buffer B (200 mM Tris and 100 mM NaCl), cells were mounted and imaged. Negative controls were obtained by transfecting the mutant PHF8 (F279S) and by repeating the procedure with no primary antibodies.

Widefield Imaging, Calcium imaging, and data analysis

Fluorescence images were obtained using a motorized inverted wide-field epifluorescence microscope (Nikon Eclipse Ti-E), using 40x and 60x Plan-Apo oil objectives, with numerical apertures of 1.35 and 1.49 respectively. Motorized excitation and emission filter wheels (Ludl electronics, Hawthorne, NY) fitted with a DAPI/CFP/YFP/DsRed quad filter set (#86010, Chroma, Rockingham, VT) were used together with filter cubes for DAPI, CFP, YFP and TxRed (Chroma) to select specific fluorescence signals. Z-stacks were obtained spanning the entire nucleus and out-of-focus fluorescence was removed using the AutoQuant deconvolution algorithm (Media Cybernetics). Calcium imaging was done either through a cell-permeable Ca^{2+}-sensitive dye (Fluo-4 AM, Invitrogen) or the transfection of a genetically encoded Ca^{2+} sensor (gCamp6, medium isoform). Images were obtained in time series of 100ms/frame, and quantification was performed through the Time Measurement feature of NIS Elements. For all purposes, Images were digitized using a cooled EM-CCD camera (iXon EM+ 885, Andor, Belfast, Northern Ireland). Image acquisition was performed using NIS Elements AR 4.2 software (Nikon). NIS Elements Binary and ROI Analysis tools were used to segment nuclei based on DAPI signal intensity.

Co-Immunoprecipitation and Western blotting

Transfected HEK293 cells growing in 6-well plates were allowed to express overnight at 37 °C to yield >90% transfection efficiency. Throughout the entire procedure, cultures and subsequent lysates were kept on ice or at 4 °C. For co-immunoprecipitation, the cultures were washed once with 1 ml of PBS, and lysed in 500 µl of lysis buffer for 30 min, then scraped into 1.5 ml tubes. Lysis buffer consisted of 5 mM HEPES pH 7.2, 0.5% NP40, 250 mM NaCl, 2 mM EDTA, 10% glycerol, 1:100 dilution of protease inhibitor cocktail (Sigma-Aldrich). The lysates were spun down for 20 min at 16,000×g to pellet cell debris. 500ul of the supernatant was then incubated on a rotator with 5 µl mouse-anti GFP(Ruiz et al.) for 90 min, followed by 100 µl of Protein-A/G Plus-Agarose (Santa Cruz Biotechnology) for another 60 min on a rotator. The beads were spun down at 1000×g for 5 min and the supernatant was removed. IP fractions were then washed and re-suspended in 1 ml lysis buffer for a total of 3 times. The beads and input lysates were resuspended and boiled at 95 °C for 5 min in sample buffer, resolved by SDS-PAGE with Tris-glycine gels (Bio-Rad), transferred to 0.2um PVDF membranes (Invitrogen), and imunoblotted. The primary antibodies used were anti-GFP (mouse-monoclonal; Roche), anti-FLAG (mouse-monoclonal; Sigma).

Immunoprecipitation and Mass Spectrometry

Immunoprecipitation was performed as above, with a pre-clearing step using 5ug of purified rabbit IgG / IP. Following the final wash step, beads were resuspended and heated to 65°C for 10 min and run on 4-20% gradient Tris-glycine gels (Bio-Rad) for 3 hours at constant 80V. Gels were stained for one hour with the GelCode Blue Stain(Ma et al.), and washed extensively with ddH2O overnight.

Using a sterile scalpel, bands that were represented in the PHF8/TIP60 IP fraction but not in the control YFP IP fraction were excised and kept in clean 1.5ml tubes, spun down at 1000×g for 5 min. Following reduction and alkylation, interacting proteins were trypsinized overnight at 37°C. Peptides were dried and resuspended in mass-spectrometry compatible buffer, and analyzed with one-dimensional nanoLC-MS/MS (Dionex UltiMate 3000 nanoLC system coupled with AB Sciex TripleTOF 5600 system) for protein identification. The IPI human protein database (version 3.77) was searched using ProteinPilot (version 4.5, AB Sciex) and the identified hits were analyzed using DAVID (http://david.abcc.ncifcrf.gov) for gene ontology annotation.

Chromatin-immunoprecipitation and Triton X-Acetic Acid-Urea histone electrophoresis

Neurons were treated with chemLTP as above; HEK293 cells growing in 6-well plates were transfected with PHF8, TIP60 or both, and allowed to express overnight at 37 °C to yield >90% transfection efficiency. DNA-protein crosslinking was done in-situ, by adding 37% Formaldehyde to growth medium to a final concentration of 1%, for 8 minutes at RT, after which the unreactive formaldehyde was quenched with 1.25M Glycine, and then washed 3x with PBS and collected. 1 million cells were lysed in 100µl of ChIP lysis buffer (1%SDS with a 1:100 dilution of protease inhibitor cocktail; Sigma-Aldrich). 10uL of unsheared input chromatin was collected, and the remaining lysates were spun down for 10 min at 10,000×g, and then sonicated for 8 cycles using the Bioruptor 2000 (Diagenode) at HIGH setting. 10 µl of unsheared and sheared chromatin were loaded on a 1% agarose gel to visualize shearing efficiency. The sheared chromatin was then diluted with ChIP dilution buffer (0.01%SDS, 1.1% Triton X, 1.2mM EDTA, 20mM Tris-HCl pH 8.0, 150mM NaCl), and DNA was quantified using a NanoDrop. 50ug of chromatin was incubated with 3 µl of the primary antibody rabbit-antiH3K4me3 (ActiveMotif) for 3 hours, followed by addition of 50µl of Protein-A/G Plus-Agarose beads (Santa Cruz Biotechnology) which is incubated for 60 min on a rotator. The beads were spun down at 1000×g for 5 min and the unbound fraction removed. IP fractions were then washed and re-suspended in three consecutive washes using the Low-Salt ChIP Wash Buffer, High-Salt ChIP Wash Buffer, and LiCl ChIP Wash Buffer (Millipore) followed by 2 final washes in TE Buffer. Immunoprecipitated chromatin was eluted, cross-links were reversed, and equal amounts of protein were loaded onto SDS-PAGE gels or Triton X-Acetic Acid-Urea (TAU) gels which were made fresh on the day of the experiment following published protocols (Shechter et al., 2007). Alternatively for ChIP-RT-PCR analyses, immunoprecipitated chromatin was eluted, reverse-crosslinked, and treated with RNAse A for 1 hour at 37°C and Proteinase K for 8 hours at 62°C. DNA was purified using a spin column (Qiagen), and eluted into 30uL volumes, out of which 2uL was used in qRT-PCR using primers against the Transcriptional Start Site (TSS) of the rat *Arc*, *BDNF, Synaptophysin,* and *Fos* genes.

3D Structured Illumination Microscopy (3D-SIM)

Neurons were treated and then fixed at the appropriate timepoints. Autofluorescence was reduced with Sodium borohydride (0.1% $NaBH_4$) for 5 minutes. Immunostaining was performed as described above, with a final wash step following secondary antibody incubation to transition the neurons into a Thiodiethanol (TDE) mounting medium. Serial dilutions of 10%, 25%, 50% and finally 97% TDE, with a final refractive index of 1.512, which directly matches that of glass, was used to mount the samples. A Zeiss Elyra PS-1 super-resolution system (Zeiss) equipped with 405, 488, 561, and 642 nm lasers (50mW, 200mW, 200mW, 150mW respectively) for excitation was used to acquire 3D-SIM images. A Zeiss 63X Plan-Apochromat (N.A=1.4) oil immersion objective lens was used with a cooled EM-CCD camera (iXon EM+ 885, Andor, Belfast, Northern Ireland) camera to capture a 1 megapixel field of view. 15 images per section per channel were acquired (made up of 3 rotations and 5 phase movements of the diffraction grating) at a z-spacing of 0.125µm. Structured illumination reconstruction and alignment was completed using the Zen software (Zeiss).

3D Stochastic Optical Reconstruction Microscopy (3D-STORM)

Neurons cultured on LabTek II chambered coverglass (thickness #1.5) were stimulated appropriately and fixed with 3% paraformaldehyde for 8 minutes, and auto-fluorescence was quenched with 0.1% $NaBH_4$ for 5 minutes. After a blocking step, immunostaining was performed as described above, with antibody concentrations titrated to the appropriate dilution. After secondary antibody incubation, antibody-antigen complexes were post-fixed with 3% paraformaldehyde, 0.1% glutaraldehyde for 5 minutes, and then washed for a total of 10 times in PBS. STORM imaging buffer containing Cysteamine (Sigma) titrated with HCl to pH 7.4 and a cocktail of Glucose-Oxidase and Catalase solution was added to aliquots of 10% glucose in PBS. 3D-STORM imaging was done on a Nikon Ti microscope equipped with a 100x Apo-TIRF oil immersion objective and an Andor iXon3 EM-CCD camera with the gain set at 200 mHz. A Coherent 488nm, Sapphire 561nm laser line operating at 150mW (Coherent) and a 647nm line with 180mW output (Obis) were used to push the Atto-488, Alexa-568, and Alexa-647 fluorophores to the triplet state, in the presence of Cysteamine HCl, Glucose Oxidase, and Catalase, in a closed environmental chamber to prevent entry of molecular oxygen. Timelapses were acquired at 50 fps, for a total of at least 15000 periods. Molecule list thresholding and 3D rendering were performed on the NIS Elements software with the STORM module installed (Nikon).

Results

The histone demethylase PHF8 colocalizes with the histone acetyltransferase TIP60 in the interchromatin space

In order to gain insight into their function, we first wanted to observe where the putative transcriptional coactivators reside in the neuronal nucleus. Endogenous and overexpressed PHF8 and TIP60 fused to spectrally non-overlapping fluorescent proteins eCFP, eYFP, mCherry, and tdTomato were imaged in primary hippocampal and cortical neurons. In all cases, PHF8 and TIP60 both localized to the nucleus, as expected (Figure 1A-F). Importantly, however, both PHF8 and TIP60 formed hundreds of tiny punctate structures of similar calibre which localized to specific regions in the nucleus that are devoid of DAPI staining, indicative of areas known as the interchromatin space, where many nuclear processes are thought to occur (Politz et al., 1999, Tycon et al., 2014). Data from widefield microscopy is supported by the higher-resolution Structured Illumination Microscopy which shows that PHF8 and TIP60 localize to the interchromatin space, which are proposed locations of transcription factories (Eskiw et al., 2008). Indeed, immunostaining of the Ser5-phosphorylated C-terminal domain of RNA Polymerase II show that this interface is rich with transcriptional initiation-specific structures in primary neuronal nuclei (Figure 1C). When expressed together in the same nucleus, we found that PHF8 tightly associated with TIP60 (Figure 1D). This observation prompted us to ask whether the overexpression of PHF8 protein may cause recruitment of TIP60 to the PHF8 puncta, and *vice versa*. To this end we transfected neurons either PHF8 or TIP60 singly and immunostained for endogenous TIP60 or PHF8 respectively and found that exogenous TIP60 puncta were rich in endogenous PHF8 (Figure 1E). Conversely, PHF8 puncta recruited endogenous TIP60 in hippocampal neurons (Figure 1F). This bi-directional recruitment suggested that PHF8 and TIP60 physically interact.

In order to investigate this protein-protein interaction in greater detail, we used P-LISA (Proximity Ligation In Situ Assay), a technique that detects interactions between molecules that are obligatorily less than 30 nm from each other (Fredriksson et al., 2002). Using an antibody against TIP60 and an antibody against the GFP-epitope of PHF8-YFP, we performed P-LISA on HEK293 cells stably transfected with PHF8-YFP to detect specific PHF8-TIP60 interactions, which formed variably sized spots that localized to the interchromatin space (Figure 1G). Using a small hairpin RNA (shRNA) to knock down the expression of endogenous PHF8, we observed that the number of P-LISA interaction hotspots was significantly reduced in cells expressing the shRNA (Figure 1H-I), suggesting that the interaction detected by proximity

ligation was specific. Immunostaining with the PHF8 antibody was performed to confirm that the interaction hotspots constituted a large majority of endogenous PHF8 puncta (Figure 1J).

PHF8 physically associates with TIP60

Despite a wealth of evidence suggesting that methylation and acetylation of histones are tightly linked, physical interactions between a histone demethylase and an acetyltransferase have not been well characterized. In light of our findings showing the co-localization of the demethylase PHF8 with the acetyltransferase TIP60 as well as their ability to recruit each other, we used a cellular system to study whether or not the two enzymes physically interact. HEK293 cells were co-transfected to >90% efficiency with TIP60-YFP and PHF8-FLAG, and their nuclear extracts were subjected to immunoprecipitation with the anti-GFP antibody to pull down TIP60-YFP. Control cells were transfected with YFP alone. After extensive rounds of washing, PHF8-FLAG remained in the IP fraction (Figure 2A) of cells transfected with TIP60-YFP, but not of cells transfected with YFP alone. Conversely, when PHF8-YFP and TIP60-FLAG were co-transfected and co-immunoprecipitation was performed, only cells that contained PHF8-YFP immunoprecipitated TIP60-FLAG, whereas control cells transfected with YFP did not (Figure 2B). In rat cortical neurons, pull-down of endogenous TIP60 with an anti-TIP60 antibody co-immunoprecipitated PHF8, whereas pull-down with anti-GFP did not (Figure 2C). To analyze which domains of TIP60 physically associated with PHF8, we performed co-immunoprecipitation experiments where full length PHF8-FLAG was co-expressed with deletion mutants of TIP60, which included the following TIP60 constructs: A (TIP60 chromo domain), B (N-terminus TIP60 including the zinc finger), C (N-terminus TIP60, excluding the Acetyl-CoA binding domain), D (containing the zinc finger and part of its MYST domain), E (C-terminus TIP60 excluding the zinc finger), and F (C-terminus TIP60 excluding the chromo domain). Our results show that PHF8 associates most strongly with TIP60 amino acids 99-546 which contains the zinc finger or putative DNA-binding domain and the active acetyltransferase MYST domain (Figure 2D, compare constructs D-F with E). In contrast, the N-terminal chromo domain, which recognizes and binds to the heterochromatin-associated H3K9me3, hindered its association with PHF8 (Figure 2D, compare constructs C with D and F).

PHF8 and TIP60 form a dual function complex that increases the acetylation of H3K4me3-bearing chromatin

The observed physical interaction between these two chromatin modifiers led us to explore whether the PHF8-TIP60 complex had any cooperative function in histone modification. We first investigated whether PHF8 and/or TIP60 had any effect on overall histone acetylation. Purified histones from HEK293 nuclear extracts obtained after transfection of PHF8, TIP60, or both were separated on Triton X-acetic acid-urea (TAU) gels. We observed that overexpression of TIP60 increases histone acetylation of H3 at lysine 9 (H3K9), but when both PHF8 and TIP60 were overexpressed, the increase in H3K9 acetylation was notably larger (Figure 2F). The same analysis was performed on total cellular histones separated on conventional SDS-PAGE gels, which shows that PHF8 and TIP60 increase total H3K9 acetylation, without affecting the loading control, total H4 (Figure 2G).

The interaction between the active chromatin mark H3K4me3 and acetylation of H3K9 and H3K14 has been well documented (Rice and Allis, 2001), but the enzymes that cooperate to cause this cross-talk are not well understood. PHF8 is a reader of the transcriptionally associated mark H3K4me3, by virtue of its PHD finger domain, while it functions to remove the repressive chromatin marks H3K9me2 and H3K9me1 (Kleine-Kohlbrecher et al., 2010, Yu et al., 2010). TIP60 is an acetyltransferase with predicted activity on many histone substrates including H3K9 and H3K14 (Kimura and Horikoshi, 1998). Following our observation that PHF8 associates with the acetyltransferase TIP60, we hypothesized that complete demethylation of H3K9me2 by PHF8 may be conducive to the acetylation of H3K9 and H3K14 in the same histone tail carrying the H3K4me3 mark. In order to test this hypothesis, we used chromatin immunoprecipitation (ChIP) to explore the possible functions of this complex on endogenous nucleosomes. We first validated the ability of our PHF8 construct to demethylate its substrate H3K9me2 using ChIP, and saw that while the wild-type enzyme was able to decrease H3K9me2, overexpression of the mutant version of PHF8-F279S, containing a single amino-acid substitution which rendered it enzymatically inactive (Feng et al., 2010), did not result in a decrease in H3K9me2 (Figure 2H). Pull-down was performed using an antibody directed against the PHF8-targeted mark H3K4me3, and the levels of acetylation at the H3K9 and H3K14 residues of these H3K4me3-positive histones were assessed by Western analysis. Consistent with its role as a histone acetyltransferase, upregulation of TIP60 expression was seen to increase acetylation of H3K9 and H3K14, but more importantly, this increase was specific to chromatin that is positive for H3K4me3. Interestingly, PHF8 overexpression by itself is also able to increase H3K9ac and H3K14ac levels. However, when both PHF8 and TIP60

316 are co-expressed, we observed an associated additive effect in the acetylation of H3 specifically in transcriptionally
317 active H3K4me3-bearing histone tails (Figure 2I-J). Taken together, both total histone gels and ChIP-TAU gels capturing
318 specifically immunoprecipitated H3K4me3 show that there is proportionately higher H3K9 and H3K14 acetylation when
319 both PHF8 and TIP60 are present, which lent further evidence that PHF8 and TIP60 may be acting cooperatively to
320 increase H3 acetylation.

321 **PHF8 removes transcriptionally suppressive H3K9me2 and associates with transcriptionally active H3K9ac**

322 Previous studies have indicated that PHF8 may be a transcriptional co-activator as it is able to demethylate the
323 transcriptionally repressive histone mark H3K9me2 in various cellular models (Loenarz et al., 2010, Suganuma and
324 Workman, 2010, Zhu et al., 2010). In the brain, the regulation of H3K9me2 has recently been found to be extremely
325 important for learning and memory (Kramer et al., 2011). After confirming that PHF8 demethylates H3K9me2 in a
326 cellular system (Figure 2H), we sought to investigate whether PHF8 is able to reduce H3K9me2 levels in primary neurons.
327 Indeed, PHF8 overexpression was sufficient to down-regulate H3K9me2 in hippocampal neurons, as seen through
328 immunofluorescence (Figure 3, compare A, B, and C). On the other hand, the clinical mutant PHF8-F279S displayed a
329 different subcellular localization and function, localizing to fewer and slightly bigger foci in the nucleus and failing to
330 down-regulate H3K9me2 (Figure 3E). In view of the interaction between PHF8 and the acetyltransferase TIP60, we
331 hypothesized that PHF8 may be regulating acetylation. We therefore screened a number of histone acetylation marks in
332 neurons and found that the PHF8 puncta were seen to associate very closely with the acetylation mark H3K9ac, a
333 transcriptionally permissive mark and known substrate of TIP60 (Kimura and Horikoshi, 1998) (Figure 3D). These findings
334 suggested that the PHF8-TIP60 complex may be responsible for mediating changes at a specific chromatin locus which
335 was H3K9, the only residue known to be able to undergo either methylation or acetylation (Zlatanova and Leuba, 2004).

336 **PHF8 and TIP60 are activity-dependent and co-regulate chromatin modification in response to neuronal activity**

337 Although neuronal activity is known to induce epigenetic modification at the level of DNA methylation (Martinowich et
338 al., 2003, Ma et al., 2009), the circumstances of activity-dependent chromatin modification is not well established. We
339 attempted to investigate this by combining a chemical Long Term Potentiation (chemLTP) paradigm which stimulates
340 network activity (Hardingham et al., 2001, Arnold et al., 2005) with a high-content imaging assay in 96-well format to

examine global activity-dependent changes in histone methylation and acetylation as a function of time. We performed a detailed time course of neuronal activation at 5, 10, 20, 40, 80 minute intervals and beyond, and found that as early as 40 minutes after increasing synaptic activity, as visualized by the genetically-encoded calcium sensor GCaMP6 (Figure 4B), expression of the activity-regulated gene *Arc* was induced (Figure 4A). Activated neurons that successfully induce ARC protein had significantly higher nuclear levels of PHF8 and TIP60 (Figure 4C and 4F, p-value < 0.0001), suggesting that both chromatin modifying enzymes are activity-dependent. In fact, a detailed time-course analysis of PHF8 and TIP60 nuclear levels in neurons that have undergone chemLTP treatment show increases in PHF8 nuclear levels which is precisely mirrored by increases in TIP60 nuclear levels within 5 minutes of synaptic activity induction (Figure 4A,C, and F). In parallel with the increases in the nuclear levels of both PHF8 and TIP60, we found that neuronal networks activated with the chemical LTP paradigm showed a robust increase in the phosphoacetylation of H3K9acS10P which was mirrored by a down-regulation of the PHF8 substrate and transcriptionally repressive mark H3K9me2 (Figure 4D), corroborating the data obtained through single-cell imaging (Figure 5) and other studies of hippocampus-dependent memory formation (Chwang et al., 2007). Amongst various histone acetylation sites tested including H3S10P, H3K9ac, H3K14ac, and H2AK5ac (Figure 4E), we observed that H3K9acS10P was most responsive to synaptic activity, with low baseline levels and consistently reproducible induction within minutes of synaptic activation, suggesting that the very early phosphoacetylation of H3K9acS10P may constitute a highly specific chromatin signature of recently activated neurons.

The PHF8-TIP60 complex modulates activity-induced H3K9S10P acetylation

Individual reports have shown that neurons are able to induce both H3S10 phosphorylation and histone acetylation in response to synaptic activity (Soriano et al., 2009, Wittmann et al., 2009), but the mechanisms by which this occurs and the possible functions of these modifications are not yet elucidated. Our observations indicate that the dual histone m ark H3K9acS10P is a highly activity-dependent chromatin modification. In order to investigate whether PHF8 and TIP60 have an effect on the occurrence of H3K9acS10P, we performed high-resolution imaging of activated neuronal nuclei. Using immunofluorescence microscopy of neurons activated with chemLTP, we validated that ARC protein, which is known to be highly regulated by activity, was induced in only a subset of the neuronal population (Figure 5a). In these

neurons that were positive for ARC, nuclear levels of endogenous TIP60 highly paralleled the increase in H3K9acS10P (Figure 5b), corroborating the results from the high-content analysis (Figure 4).

We then asked if PHF8 could affect this increase in the activity-dependent acetylation of H3K9acS10P. To answer this question, we transfected neurons with either wild-type PHF8 or the clinical mutant PHF8-F279S, and imaged them after chemLTP induction. Staining for both ARC and H3K9acS10P indicated that neurons with increased PHF8 have significantly higher H3K9acS10P and a higher probability of ARC protein expression (Figure 5C-D). On the other hand, knockdown of PHF8 through transfection of two shRNAs significantly decreases H3K9acS10P (Figure 6A). In order to more accurately delineate this interaction and to circumvent the problem that we could only visualize 3 proteins at a time immunohistochemically, we performed Structured Illumination Microscopy which revealed that the complex containing PHF8 and TIP60 directly associated with H3K9acS10P in the activated neuronal nucleus (Figure 5E).

Time-course chromatin immunoprecipitation of neurons activated by chemLTP and showed that while H3K9me2 levels decreased at the *Arc* TSS, H3K9acS10P was massively upregulated within 10 minutes of synaptic activity (Figure 7A-B). ChIP analyses of rapid early recruitment of PHF8 and TIP60 to the *Arc* TSS (Figure 7C-D). which coincided with a surge in H3K9acS10P phosphoacetylation at the same genomic locus (Figure 7B) that was not seen in other activity-dependent gene promoters and control genomic loci. Thus, taken together with the results obtained from high-content imaging, time-course ChIP data seems to suggest that the nuclear reorganization and active recruitment of PHF8 and TIP60 protein into gene promoters may be a possible mechanism by which neural activity causes changes in histone acetylation and methylation status that in turn influence the transcription of neuronal genes such as *Arc*.

The PHF8-TIP60 interactome is rich in proteins involved in transcription and includes the neuronal splicing factor PSF

The identification of an activity-dependent chromatin modifying complex may have wide-ranging implications in neuronal functions. We sought to investigate the possible functions of PHF8 and TIP60 by examining the protein partners they interact with. Both PHF8 and TIP60 have been implicated in various aspects of neuronal function and gene transcription (Kleine-Kohlbrecher et al., 2010, Tea and Luo, 2011), but a low-bias view of the PHF8-TIP60 interactome has not been established. We therefore performed immunoprecipitation followed by mass spectrometry of nuclear

extracts from Hek293T cells transfected with PHF8-YFP or TIP60-YFP. The immunoprecipitates were run on a gel stained with Coomassie blue and bands were excised for mass spectrometric analysis. A large majority of the proteins which were found to immunoprecipitate with PHF8 and TIP60 had functions in transcription, splicing, and RNA processing (Figure 8). Amongst the top interactors that were prominently represented by both the PHF8 and TIP60 IP-MS were the splicing factor SFPQ, also known as Polypyrimidine tract-binding protein-associated Splicing Factor (PSF) and its partner NONO, as well as several ATP-dependent RNA helicases including DDX17, DDX21, and DDX3X, which strongly suggested that PHF8 and TIP60 may be functioning in transcription-related processes.

Endogenous PHF8, TIP60, and PSF are found within 30 nm of each other in the activated neuronal nucleus

Although PHF8 and TIP60 are found to tightly co-localize when viewed using conventional immunofluorescence microscopy, it remains difficult to ascertain precisely how these chromatin modifying enzymes are positioned relative to each other in the nucleus as the resolution of a conventional light microscopy is limited to 250 nm, nearly twenty times the diameter of a single nucleosome (11 nm). To overcome this hurdle, we employed 3D-STORM (3-Dimensional Stochastic Optical Reconstruction Microscopy), which has a resolution limit of 20 nm, allowing us to directly observe endogenous PHF8 and TIP60 interactions at the single molecule level. Indeed as suggested by proximity ligation, single-molecule imaging by STORM shows that a large majority of PHF8 proteins were found to associate with TIP60 (Figure 9). Within the interaction hotspots, PHF8 and TIP60 were found to co-localize in an interaction radius of 20 nm (Figure 9A), which is less than the diameter of the 30 nm packed chromatin fibre, demonstrating for the first time the association of a histone demethylase and an acetyltransferase at level of a single nucleosome. As we had the capability to view these complexes three-dimensionally we were able to observe that the single-molecule interaction between PHF8 and TIP60 did not occur in a random orientation, but rather had a specific spatial relationship (Figure 9B; compare the projections in the xy, xz, and yz planes). Interestingly, we observed that molecules of PHF8 and TIP60 were found to form a linearly well-defined interface, which prompted us to investigate what may be lying within. We investigated several candidate proteins garnered through the IP-MS screen (Figure 8), and found that the splicing factor PSF was situated at this interface between PHF8 and TIP60: tri-color 3-D STORM imaging shows that PHF8, TIP60 and PSF form a well-defined tri-partite complex in the neuronal nucleus (Figure 10A-C, Movie 1).

Discussion

Chromatin modification has a major role in the generation of complex behaviors such as learning and memory (Alarcon et al., 2004, Peixoto and Abel, 2013). Paradigms of memory formation such as contextual fear conditioning induces changes in neuronal transcriptional programs through dramatic alterations of chromatin structure (Gupta et al., 2010, Bousiges et al., 2013), yet the mechanisms by which chromatin-modifying enzymes regulate gene expression in response to neuronal activity are still unclear (Roth and Sweatt, 2009, Vogel-Ciernia and Wood, 2013). Here we show that the activity-dependent induction of memory consolidation genes is facilitated by a novel dual function chromatin-modifying complex. Specifically, demethylation of the transcriptionally suppressive H3K9me2 mark is linked to the acetylation of H3 through a specific interaction between the H3K9me2-specific X-linked mental retardation protein PHF8 and the Alzheimer's disease-associated TIP60. Results presented in this study indicate that the PHF8-TIP60 complex may function as an epigenetic initiator of rapid *Arc* gene induction likely by interacting with mRNA processing proteins such as the neuronal splicing factor PSF and by upregulating H3K9acS10P, a chromatin modification that highly favors transcriptional elongation at the *Arc* transcriptional start site.

A chromatin-modifiying complex that regulates histone methylation and acetylation in response to synaptic activity

Neuronal cells respond to environmental cues by altering chromatin signatures that affect gene transcription (Crosio et al., 2003). Whether or not specific histone marks are involved in transcriptional activation is the subject of intense research. Histone acetylation is thought to be a transcriptionally permissive modification which is important in memory formation (Peixoto and Abel, 2013), while histone methylation may be activating or repressive (Jarome and Lubin, 2013). It has been known for a long time that both modifications are related to transcription (Allfrey et al., 1964) and recent evidence suggests that histone acetylation and methylation may be regulated cooperatively to activate transcription (Latham and Dent, 2007). For instance, histone acetylation correlates strongly with methylation in the context of gene induction (Zhang et al., 2004, Nightingale et al., 2007). In hippocampal neurons, electroconvulsive seizures induce changes in transcription by altering chromatin acetylation and methylation in a locus-specific manner (Tsankova et al.,

2004). Nevertheless, little is known about how the enzymes responsible for acetylation and methylation cooperate and which chromatin modifications, if any, are required for neuronal gene transcription.

Studies done in *Drosophila* and mammals support the evolutionarily conserved role of a particular histone methylation mark, H3K9me2, in learning and memory (Gupta-Agarwal et al., 2014). PHF8 is a H3K9me2-specific histone demethylase that is clinically found to be mutated in a severe form of X-linked mental retardation (Laumonnier et al., 2005). PHF8 possesses a Plant Homeo Domain (PHD) finger domain targeting it to transcriptional start sites, and a Jumonji catalytic domain which is capable of removing the transcriptionally repressive mark H3K9me2/1 and H4K20me1 (Qi et al., 2010). The role of PHF8 mutations in causing mental retardation has been attributed to the inability of mutant PHF8 to activate ribosomal DNA transcription (Feng et al., 2010). Other studies suggest that PHF8 is a positive regulator of mRNA transcription, as it physically associates with RNA Polymerase II along with transcription factors such as c-Myc and E2F (Asensio-Juan et al., 2012). Like PHF8, TIP60 has been found to be recruited to chromatin by c-Myc and E2F, where it has a function in transcriptional activation of both ribosomal and messenger RNA (Sapountzi et al., 2006). Although it has an emerging neurological phenotype (Lorbeck et al., 2011) and has been implicated in the pathogenesis of Alzheimer's disease (Cao and Sudhof, 2001), TIP60 has no currently known function in activity-dependent gene induction.

We report evidence that both PHF8 and TIP60 are located in the interchromatin space where transcription is thought to occur (Tycon et al., 2014). PHF8 shows a unique sub-nuclear distribution constituting a large number of small puncta, whose localization overlapped robustly with that of the acetyltransferase TIP60 (Figure 1d). Furthermore, exogenous PHF8 is seen to recruit endogenous TIP60 and *vice versa*, while proximity ligation and co-immunoprecipitation experiments both demonstrate that PHF8 interacts with TIP60. This physical interaction and the observation that overexpression of a demethylase increases histone acetylation prompted us to ask whether PHF8 and TIP60 may be cooperatively modifying chromatin. Cross-talk between histone acetylation and methylation has been noted to be biologically significant (Kennedy et al., 2013), yet the interaction between demethylation and acetylation, along with the identity of the enzymes responsible for these changes are still unknown. The data presented here shows that PHF8 and TIP60 increase H3 acetylation predominantly on transcriptionally permissive H3K4me3-bearing chromatin, suggesting that the increase in acetylation may be specific to transcriptionally active genomic locations.

Given the identification of a complex that is capable of cooperatively modifying chromatin, we now address the issue of which specific histone marks may be regulated in response to neuronal activity. We observed that PHF8, but not the clinical mutant PHF8-F279S, is able to specifically downregulate the transcriptionally suppressive histone mark H3K9me2, consistent with its role as a transcriptional co-activator. However, besides removing H3K9me2, PHF8 tightly associates with H3K9ac, an important histone mark that is associated with paused RNA Polymerase II (Margaritis and Holstege, 2008). This unexpected association was the first clue that demethylation and acetylation may be linked in neurons, specifically at the H3K9 epigenetic locus. Besides being implicated in evolutionarily conserved roles of learning and memory, the H3K9 locus is peculiar in that it can be acetylated or methylated, often with opposing biological consequences. In order to examine which histone marks are activity-regulated, we used a high-content screening platform to observe epigenetic changes at the network level, where we found that a treatment paradigm consisting of 4-aminopyridine, Bicuculline, and Forskolin, which has been shown to increase synaptic activity and cause LTP (Otmakhov et al., 2004), increases nuclear levels of PHF8 and TIP60 protein specifically in neurons that succesfully induce the immediate-early gene *Arc* (Figure 4A-C). Consistent with the increase in PHF8, we found that activity transiently downregulated the PHF8 substrate H3K9me2 (Figure 4D). To our surprise, while immunostaining with the H3K9ac and H3K14ac antibodies did not show a robust regulation with regard to activity (Figure 4E), we detected a highly specific activity-regulated increase in the dual histone mark H3K9acS10P (Figure 4D), suggesting that a highly specific chromatin switch may exist in the bivalent H3K9 residue, but only in the context of S10 phosphorylation. Our findings thus characterize H3K9acS10P as an epigenetic chromatin signature that is faithfully produced by synaptic activity. The importance of the dual-mark H3K9acS10P is corroborated by previous reports which show that contextual fear conditioning and novel environment exposure induced changes in H3S10 phosphorylation, H3 acetylation and H3K9me2 demethylation (Levenson et al., 2004, Chwang et al., 2006, Gupta et al., 2010, Gupta-Agarwal et al., 2014). A direct mechanism of combinatorial histone modification proposed by our study is that demethylation of the H3K9 residue by PHF8 in turn allows for its acetylation by TIP60 in the dual function complex which may happen concurrently with or following the phosphorylation of the adjacent H3S10 (Duan et al., 2008). Further research is needed to optimally dissect the pathways that converge on H3S10 phosphorylation and the role that PHF8-TIP60 may play in this process.

Regulation of neuronal gene transcription by H3K9acS10P, a chromatin modification specific for transcriptional elongation

What could be the function of this neuronal activity-regulated chromatin modification complex? Clinically, mutations in PHF8 protein that render it enzymatically inactive cause severe cognitive deficits (Laumonnier et al., 2005, Loenarz et al., 2010). While no known clinical mutation in TIP60 has yet been reported, nervous system-specific loss of TIP60 acetyltransferase activity dramatically worsens the Alzheimer's disease phenotype in *Drosophila* (Pirooznia et al., 2012, Johnson et al., 2013, Xu et al., 2014). Furthermore, recent research shows that both PHF8 and TIP60 have important roles in transcriptional elongation (Halkidou et al., 2004, Wang et al., 2009, Mahajan and Stanley, 2014). Taken together, these evidence strongly point toward a role for PHF8 and TIP60 in transcriptional activation.

Given our current findings, we postulate that the PHF8-TIP60 complex may be functioning to increase the expression of neuronal genes such as *Arc* through the enzymatic modulation of H3K9acS10P, which is a highly important chromatin modification that mediates transcriptional elongation (Macdonald et al., 2005, Winter et al., 2008, Zippo et al., 2009, Karam et al., 2010, Li et al., 2013). Three lines of reasoning led to this conclusion: first, PHF8 and TIP60 nuclear levels paralleled the activity-dependent increase of H3K9acS10P and the surge in the expression of *Arc*, which became upregulated from extremely low baseline levels. Second, overexpression of PHF8 significantly enhanced the formation of H3K9acS10P and ARC protein, whereas the X-linked mental retardation mutant PHF8-F279S failed to produce the same effect, indicating that the demethylase activity of PHF8 is critical. Consistent with this view, inhibition of PHF8 gene expression using two different shRNAs significantly decreased H3K9acS10P induction. Third, using high-resolution Structured Illumination Microscopy, we directly show that both PHF8 and TIP60 are tightly bound to H3K9acS10P. In summary, neuronal PHF8 and TIP60 may influence gene transcription by acting as activity-dependent writers of H3K9ac, which is known to be upregulated in novel environment exposure (Bousiges et al., 2013) and fear conditioning (Peleg et al., 2010), but only in the context of H3S10 phosphorylation, which has previously been shown to be critical for associative memory (Levenson and Sweatt, 2005).

The link between H3K9acS10P and transcription has been made in light of recent evidence showing that H3K9acS10P is required for transcriptional elongation through recruitment of the double bromodomain enzyme BRD4 and the

elongation factor pTEF-b (Ong and Corces, 2011). Here we show that in neurons, PHF8, TIP60, and H3K9acS10P were found to be specifically enriched in the *Arc* TSS in an activity-dependent manner (Figure 7B-D). An intriguing possibility raised by this study is that upregulation of H3K9acS10P by PHF8 and TIP60 may serve as the initial impetus that transduces synaptic activity to the nucleus to drive the rapid transcription of *Arc*, which is poised for near-instantaneous transcription through promoter-proximal Pol II stalling (Saha et al., 2011). It is worth noting that the highly rapid transcriptional activation through release of Pol II into the elongation state is a conserved and well-characterized mechanism of gene induction (Hargreaves et al., 2009). By allowing for the locus-specific formation of H3K9acS10P which may serve as a platform for binding of elongation factors, the PHF8-TIP60 complex may be tipping the scale in favor of transcriptional elongation in response to synaptic activity.

Further evidence implicating this complex in the active transcriptional process is our finding that an overwhelming majority of the binding partners of PHF8 and TIP60 consisted of proteins involved in mRNA splicing and processing (Figure 8). One highly represented protein in the PHF8-TIP60 interactome is the RNA Polymerase II-associated splicing factor PSF (Polypyrimidine tract-binding protein-associated Splicing Factor) (Emili et al., 2002, Rosonina et al., 2005), which is reported to play a key role in neuronal development (Lowery et al., 2007), alternative splicing (Kim et al., 2011), and is found to be dysregulated in neurodegenerative diseases (Ke et al., 2012). Although the interaction between PHF8 and PSF may be partly explained by the affinity of these proteins to the C-terminal domain of RNA Polymerase II (Fortschegger et al., 2010), the highly structured molecular interaction between PHF8, TIP60, and the splicing factor PSF (Figure 10) points towards a transcriptional role for the PHF8-TIP60 complex and supports the idea that pre-mRNA processing may be occuring co-transcriptionally (Ameur et al., 2011, Lee and Tarn, 2013, Bentley, 2014) .

In an attempt to directly observe this neuronal activity-regulated chromatin-modifying complex, we characterized the PHF8-TIP60 interaction in the neuronal nucleus at the single-molecule level using the single-molecule imaging technique 3D-STORM (Rust et al., 2006, Huang et al., 2008). Analysis at super-resolution reveals that interactions that are reportedly overlapping at the resolution of conventional light microscopy may be more complex than they seem, as we see PHF8 and TIP60 molecules not colocalizing perfectly but rather tightly associating with each other in an interaction radius of less than 20 nm, which comes increasingly close to the resolution needed to observe the “beads on a string”

structure of nucleosomes on which general transcription is thought to occur (Smolle and Venkatesh, 2014). It was only upon 3-dimensional rendering, however, that we see these chromatin-modifying enzymes interacting in a well-defined spatial orientation with a clear interphase (Figure 9B). Intriguingly, consistent with IP-MS data, our work using 3-color 3-D STORM situates the splicing factor PSF in the middle of this interface between PHF8 and TIP60 (Figure 10), offering a glimpse into the mechanism of co-transcriptional splicing in activated neuronal nuclei.

Could a chromatin mark such as H3K9acS10P serve as a regulator of memory formation processes through the modulation of transcription? If so, can the ability of neurons to change chromatin structure be altered enzymatically to facilitate or inhibit activity-dependent gene induction? The findings summarized in this report point to a mechanism by which synaptic activity may be transduced into the nucleus as an early epigenetic event that mediates downstream processes such as transcription. PHF8 is unique in that it has a PHD domain that is specific for transcriptionally active H3K4me3 coupled to demethylase activity against transcriptionally suppressive H3K9me2/1 and H4K20me (Vermeulen et al., 2010) making it well-suited to be a transcriptional activator (Perner and Chung, 2013). Transcription elongation, however, requires extensive histone acetylation of residues such as H3K9 and H4K16 which serve as nucleosomal binding sites for BRD-4 to increase RNA Pol II processivity (Zippo et al., 2009). By associating with the histone acetyltransferase TIP60 and activating histone acetylation in a highly targeted manner, PHF8 may indeed serve as the link between transcription initiation and elongation. A possible mechanism which may therefore be proposed is that rapid phosphoacetylation of H3K9acS10P by activity-dependent PHF8 and TIP60 may promote the escape of stalled RNA Polymerase II and thereby transcription of immediate-early genes. A direct consequence from such a proposal is that abrogation of PHF8 function would prove to be detrimental towards learning-induced neuronal H3K9acS10P formation and the resulting neuroplasticity-related gene expression programs. Hence, the findings described here at least partly explains the limited capability to consolidate memories seen in patients who lack functional PHF8, and instigates further research into the possibility of altering activity-dependent gene transcription by modulation of epigenetic enzymes.

In summary, this work supports the idea that a neuronal dual-function chromatin modifying complex containing PHF8 and TIP60 may serve as an epigenetic gateway to memory formation processes by regulating H3K9acS10P, a learning-induced, activity-dependent chromatin mark that enables *de novo* activity-dependent gene transcription. Future

research into the modulation of epigenetic enzymes such as these may have potential applications in the development of novel therapeutics for disorders of learning and memory.

References

Alarcon JM, Malleret G, Touzani K, Vronskaya S, Ishii S, Kandel ER, Barco A (2004) Chromatin acetylation, memory, and LTP are impaired in CBP+/- mice: a model for the cognitive deficit in Rubinstein-Taybi syndrome and its amelioration. Neuron 42:947-959.

Allfrey VG, Faulkner R, Mirsky AE (1964) Acetylation and Methylation of Histones and Their Possible Role in the Regulation of Rna Synthesis. Proc Natl Acad Sci U S A 51:786-794.

Ameur A, Zaghlool A, Halvardson J, Wetterbom A, Gyllensten U, Cavelier L, Feuk L (2011) Total RNA sequencing reveals nascent transcription and widespread co-transcriptional splicing in the human brain. Nature structural & molecular biology 18:1435-1440.

Antunes-Martins A, Mizuno K, Irvine EE, Lepicard EM, Giese KP (2007) Sex-dependent up-regulation of two splicing factors, Psf and Srp20, during hippocampal memory formation. Learn Mem 14:693-702.

Arnold FJ, Hofmann F, Bengtson CP, Wittmann M, Vanhoutte P, Bading H (2005) Microelectrode array recordings of cultured hippocampal networks reveal a simple model for transcription and protein synthesis-dependent plasticity. J Physiol 564:3-19.

Asensio-Juan E, Gallego C, Martinez-Balbas MA (2012) The histone demethylase PHF8 is essential for cytoskeleton dynamics. Nucleic acids research 40:9429-9440.

Bentley DL (2014) Coupling mRNA processing with transcription in time and space. Nature reviews Genetics 15:163-175.

Bloomer WA, VanDongen HM, VanDongen AM (2007) Activity-regulated cytoskeleton-associated protein Arc/Arg3.1 binds to spectrin and associates with nuclear promyelocytic leukemia (PML) bodies. Brain Res 1153:20-33.

Bousiges O, Neidl R, Majchrzak M, Muller MA, Barbelivien A, Pereira de Vasconcelos A, Schneider A, Loeffler JP, Cassel JC, Boutillier AL (2013) Detection of histone acetylation levels in the dorsal hippocampus reveals early tagging on specific residues of H2B and H4 histones in response to learning. PLoS One 8:e57816.

Cao X, Sudhof TC (2001) A transcriptionally [correction of transcriptively] active complex of APP with Fe65 and histone acetyltransferase Tip60. Science 293:115-120.

Chwang WB, Arthur JS, Schumacher A, Sweatt JD (2007) The nuclear kinase mitogen- and stress-activated protein kinase 1 regulates hippocampal chromatin remodeling in memory formation. J Neurosci 27:12732-12742.

Chwang WB, O'Riordan KJ, Levenson JM, Sweatt JD (2006) ERK/MAPK regulates hippocampal histone phosphorylation following contextual fear conditioning. Learn Mem 13:322-328.

Crosio C, Heitz E, Allis CD, Borrelli E, Sassone-Corsi P (2003) Chromatin remodeling and neuronal response: multiple signaling pathways induce specific histone H3 modifications and early gene expression in hippocampal neurons. J Cell Sci 116:4905-4914.

Day JJ, Sweatt JD (2011) Epigenetic mechanisms in cognition. Neuron 70:813-829.

Duan Q, Chen H, Costa M, Dai W (2008) Phosphorylation of H3S10 blocks the access of H3K9 by specific antibodies and histone methyltransferase. Implication in regulating chromatin dynamics and epigenetic inheritance during mitosis. J Biol Chem 283:33585-33590.

Emili A, Shales M, McCracken S, Xie W, Tucker PW, Kobayashi R, Blencowe BJ, Ingles CJ (2002) Splicing and transcription-associated proteins PSF and p54nrb/nonO bind to the RNA polymerase II CTD. RNA 8:1102-1111.

Eskiw CH, Rapp A, Carter DR, Cook PR (2008) RNA polymerase II activity is located on the surface of protein-rich transcription factories. Journal of cell science 121:1999-2007.

Feng W, Yonezawa M, Ye J, Jenuwein T, Grummt I (2010) PHF8 activates transcription of rRNA genes through H3K4me3 binding and H3K9me1/2 demethylation. Nature structural & molecular biology 17:445-450.

Fortschegger K, de Graaf P, Outchkourov NS, van Schaik FM, Timmers HT, Shiekhattar R (2010) PHF8 targets histone methylation and RNA polymerase II to activate transcription. Mol Cell Biol 30:3286-3298.

Fredriksson S, Gullberg M, Jarvius J, Olsson C, Pietras K, Gustafsdottir SM, Ostman A, Landegren U (2002) Protein detection using proximity-dependent DNA ligation assays. Nature biotechnology 20:473-477.

Gupta-Agarwal S, Jarome TJ, Fernandez J, Lubin FD (2014) NMDA receptor- and ERK-dependent histone methylation changes in the lateral amygdala bidirectionally regulate fear memory formation. Learn Mem 21:351-362.

Gupta S, Kim SY, Artis S, Molfese DL, Schumacher A, Sweatt JD, Paylor RE, Lubin FD (2010) Histone methylation regulates memory formation. J Neurosci 30:3589-3599.

620 Halkidou K, Logan IR, Cook S, Neal DE, Robson CN (2004) Putative involvement of the histone acetyltransferase Tip60 in
621 ribosomal gene transcription. Nucleic acids research 32:1654-1665.
622 Hardingham GE, Arnold FJ, Bading H (2001) Nuclear calcium signaling controls CREB-mediated gene expression triggered
623 by synaptic activity. Nat Neurosci 4:261-267.
624 Hargreaves DC, Horng T, Medzhitov R (2009) Control of inducible gene expression by signal-dependent transcriptional
625 elongation. Cell 138:129-145.
626 Huang B, Jones SA, Brandenburg B, Zhuang X (2008) Whole-cell 3D STORM reveals interactions between cellular
627 structures with nanometer-scale resolution. Nature methods 5:1047-1052.
628 Inoue M, Yagishita-Kyo N, Nonaka M, Kawashima T, Okuno H, Bito H (2010) Synaptic activity-responsive element (SARE):
629 A unique genomic structure with an unusual sensitivity to neuronal activity. Communicative & integrative
630 biology 3:443-446.
631 Jarome TJ, Lubin FD (2013) Histone lysine methylation: critical regulator of memory and behavior. Rev Neurosci 24:375-
632 387.
633 Johnson AA, Sarthi J, Pirooznia SK, Reube W, Elefant F (2013) Increasing Tip60 HAT Levels Rescues Axonal Transport
634 Defects and Associated Behavioral Phenotypes in a Drosophila Alzheimer's Disease Model. J Neurosci 33:7535-
635 7547.
636 Karam CS, Kellner WA, Takenaka N, Clemmons AW, Corces VG (2010) 14-3-3 mediates histone cross-talk during
637 transcription elongation in Drosophila. PLoS genetics 6:e1000975.
638 Ke YD, Dramiga J, Schutz U, Kril JJ, Ittner LM, Schroder H, Gotz J (2012) Tau-mediated nuclear depletion and cytoplasmic
639 accumulation of SFPQ in Alzheimer's and Pick's disease. PLoS One 7:e35678.
640 Kennedy PJ, Feng J, Robison AJ, Maze I, Badimon A, Mouzon E, Chaudhury D, Damez-Werno DM, Haggarty SJ, Han MH,
641 Bassel-Duby R, Olson EN, Nestler EJ (2013) Class I HDAC inhibition blocks cocaine-induced plasticity by targeted
642 changes in histone methylation. Nat Neurosci 16:434-440.
643 Kim KK, Kim YC, Adelstein RS, Kawamoto S (2011) Fox-3 and PSF interact to activate neural cell-specific alternative
644 splicing. Nucleic acids research 39:3064-3078.
645 Kim TK, Hemberg M, Gray JM, Costa AM, Bear DM, Wu J, Harmin DA, Laptewicz M, Barbara-Haley K, Kuersten S,
646 Markenscoff-Papadimitriou E, Kuhl D, Bito H, Worley PF, Kreiman G, Greenberg ME (2010) Widespread
647 transcription at neuronal activity-regulated enhancers. Nature 465:182-187.
648 Kimura A, Horikoshi M (1998) Tip60 acetylates six lysines of a specific class in core histones in vitro. Genes Cells 3:789-
649 800.
650 Kleine-Kohlbrecher D, Christensen J, Vandamme J, Abarrategui I, Bak M, Tommerup N, Shi X, Gozani O, Rappsilber J,
651 Salcini AE, Helin K (2010) A functional link between the histone demethylase PHF8 and the transcription factor
652 ZNF711 in X-linked mental retardation. Mol Cell 38:165-178.
653 Koivisto AM, Ala-Mello S, Lemmela S, Komu HA, Rautio J, Jarvela I (2007) Screening of mutations in the PHF8 gene and
654 identification of a novel mutation in a Finnish family with XLMR and cleft lip/cleft palate. Clinical genetics
655 72:145-149.
656 Kramer JM, Kochinke K, Oortveld MA, Marks H, Kramer D, de Jong EK, Asztalos Z, Westwood JT, Stunnenberg HG,
657 Sokolowski MB, Keleman K, Zhou H, van Bokhoven H, Schenck A (2011) Epigenetic regulation of learning and
658 memory by Drosophila EHMT/G9a. PLoS Biol 9:e1000569.
659 Latham JA, Dent SY (2007) Cross-regulation of histone modifications. Nature structural & molecular biology 14:1017-
660 1024.
661 Laumonnier F, Holbert S, Ronce N, Faravelli F, Lenzner S, Schwartz CE, Lespinasse J, Van Esch H, Lacombe D, Goizet C,
662 Phan-Dinh Tuy F, van Bokhoven H, Fryns JP, Chelly J, Ropers HH, Moraine C, Hamel BC, Briault S (2005)
663 Mutations in PHF8 are associated with X linked mental retardation and cleft lip/cleft palate. Journal of medical
664 genetics 42:780-786.
665 Lee KM, Tarn WY (2013) Coupling pre-mRNA processing to transcription on the RNA factory assembly line. RNA biology
666 10:380-390.
667 Levenson JM, O'Riordan KJ, Brown KD, Trinh MA, Molfese DL, Sweatt JD (2004) Regulation of histone acetylation during
668 memory formation in the hippocampus. The Journal of biological chemistry 279:40545-40559.
669 Levenson JM, Sweatt JD (2005) Epigenetic mechanisms in memory formation. Nature reviews Neuroscience 6:108-118.

Lewis PN, Lukiw WJ, De Boni U, McLachlan DR (1981) Changes in chromatin structure associated with Alzheimer's disease. Journal of neurochemistry 37:1193-1202.

Li G, White CA, Lam T, Pone EJ, Tran DC, Hayama KL, Zan H, Xu Z, Casali P (2013) Combinatorial H3K9acS10ph histone modification in IgH locus S regions targets 14-3-3 adaptors and AID to specify antibody class-switch DNA recombination. Cell reports 5:702-714.

Loenarz C, Ge W, Coleman ML, Rose NR, Cooper CD, Klose RJ, Ratcliffe PJ, Schofield CJ (2010) PHF8, a gene associated with cleft lip/palate and mental retardation, encodes for an Nepsilon-dimethyl lysine demethylase. Hum Mol Genet 19:217-222.

Lopez-Atalaya JP, Barco A (2014) Can changes in histone acetylation contribute to memory formation? Trends Genet 30:529-539.

Lorbeck M, Pirooznia K, Sarthi J, Zhu X, Elefant F (2011) Microarray analysis uncovers a role for Tip60 in nervous system function and general metabolism. PLoS One 6:e18412.

Lowery LA, Rubin J, Sive H (2007) Whitesnake/sfpq is required for cell survival and neuronal development in the zebrafish. Developmental dynamics : an official publication of the American Association of Anatomists 236:1347-1357.

Lubin FD, Gupta S, Parrish RR, Grissom NM, Davis RL (2011) Epigenetic Mechanisms: Critical Contributors to Long-Term Memory Formation. The Neuroscientist : a review journal bringing neurobiology, neurology and psychiatry.

Ma DK, Jang MH, Guo JU, Kitabatake Y, Chang ML, Pow-Anpongkul N, Flavell RA, Lu B, Ming GL, Song H (2009) Neuronal activity-induced Gadd45b promotes epigenetic DNA demethylation and adult neurogenesis. Science 323:1074-1077.

Ma H, Liu Q, Diamond SL, Pierce EA (2004) Mouse embryonic stem cells efficiently lipofected with nuclear localization peptide result in a high yield of chimeric mice and retain germline transmission potency. Methods 33:113-120.

Macdonald N, Welburn JP, Noble ME, Nguyen A, Yaffe MB, Clynes D, Moggs JG, Orphanides G, Thomson S, Edmunds JW, Clayton AL, Endicott JA, Mahadevan LC (2005) Molecular basis for the recognition of phosphorylated and phosphoacetylated histone h3 by 14-3-3. Mol Cell 20:199-211.

Mahajan MA, Stanley FM (2014) Insulin-activated Elk-1 recruits the TIP60/NuA4 complex to increase prolactin gene transcription. Molecular and cellular endocrinology 382:159-169.

Margaritis T, Holstege FC (2008) Poised RNA polymerase II gives pause for thought. Cell 133:581-584.

Martinowich K, Hattori D, Wu H, Fouse S, He F, Hu Y, Fan G, Sun YE (2003) DNA methylation-related chromatin remodeling in activity-dependent BDNF gene regulation. Science 302:890-893.

Nightingale KP, Gendreizig S, White DA, Bradbury C, Hollfelder F, Turner BM (2007) Cross-talk between histone modifications in response to histone deacetylase inhibitors - MLL4 links histone H3 acetylation and histone H3K4 methylation. Journal of Biological Chemistry 282:4408-4416.

Ong CT, Corces VG (2011) Enhancer function: new insights into the regulation of tissue-specific gene expression. Nature reviews Genetics 12:283-293.

Otmakhov N, Khibnik L, Otmakhova N, Carpenter S, Riahi S, Asrican B, Lisman J (2004) Forskolin-induced LTP in the CA1 hippocampal region is NMDA receptor dependent. J Neurophysiol 91:1955-1962.

Peixoto L, Abel T (2013) The role of histone acetylation in memory formation and cognitive impairments. Neuropsychopharmacology 38:62-76.

Peleg S, Sananbenesi F, Zovoilis A, Burkhardt S, Bahari-Javan S, Agis-Balboa RC, Cota P, Wittnam JL, Gogol-Doering A, Opitz L, Salinas-Riester G, Dettenhofer M, Kang H, Farinelli L, Chen W, Fischer A (2010) Altered histone acetylation is associated with age-dependent memory impairment in mice. Science 328:753-756.

Perner J, Chung H-R (2013) Chromatin signaling and transcription initiation. Frontiers in Life Science 7:22-30.

Pirooznia SK, Sarthi J, Johnson AA, Toth MS, Chiu K, Koduri S, Elefant F (2012) Tip60 HAT activity mediates APP induced lethality and apoptotic cell death in the CNS of a Drosophila Alzheimer's disease model. PLoS One 7:e41776.

Politz JC, Tuft RA, Pederson T, Singer RH (1999) Movement of nuclear poly(A) RNA throughout the interchromatin space in living cells. Current biology : CB 9:285-291.

Qi HH, Sarkissian M, Hu GQ, Wang Z, Bhattacharjee A, Gordon DB, Gonzales M, Lan F, Ongusaha PP, Huarte M, Yaghi NK, Lim H, Garcia BA, Brizuela L, Zhao K, Roberts TM, Shi Y (2010) Histone H4K20/H3K9 demethylase PHF8 regulates zebrafish brain and craniofacial development. Nature 466:503-507.

720 Rice JC, Allis CD (2001) Histone methylation versus histone acetylation: new insights into epigenetic regulation. Current
721 opinion in cell biology 13:263-273.
722 Ronan JL, Wu W, Crabtree GR (2013) From neural development to cognition: unexpected roles for chromatin. Nature
723 reviews Genetics 14:347-359.
724 Rosonina E, Ip JY, Calarco JA, Bakowski MA, Emili A, McCracken S, Tucker P, Ingles CJ, Blencowe BJ (2005) Role for PSF in
725 mediating transcriptional activator-dependent stimulation of pre-mRNA processing in vivo. Mol Cell Biol
726 25:6734-6746.
727 Roth TL, Sweatt JD (2009) Regulation of chromatin structure in memory formation. Current opinion in neurobiology
728 19:336-342.
729 Ruiz S, Panopoulos AD, Montserrat N, Multon MC, Daury A, Rocher C, Spanakis E, Batchelder EM, Orsini C, Deleuze JF,
730 Izpisua Belmonte JC (2012) Generation of a drug-inducible reporter system to study cell reprogramming in
731 human cells. The Journal of biological chemistry 287:40767-40778.
732 Rust MJ, Bates M, Zhuang X (2006) Sub-diffraction-limit imaging by stochastic optical reconstruction microscopy
733 (STORM). Nature methods 3:793-795.
734 Saha RN, Wissink EM, Bailey ER, Zhao M, Fargo DC, Hwang JY, Daigle KR, Fenn JD, Adelman K, Dudek SM (2011) Rapid
735 activity-induced transcription of Arc and other IEGs relies on poised RNA polymerase II. Nat Neurosci 14:848-856.
736 Sapountzi V, Logan IR, Robson CN (2006) Cellular functions of TIP60. The international journal of biochemistry & cell
737 biology 38:1496-1509.
738 Sen N (2014) Epigenetic Regulation of Memory by Acetylation and Methylation of Chromatin: Implications in
739 Neurological Disorders, Aging, and Addiction. Neuromolecular Med.
740 Shechter D, Dormann HL, Allis CD, Hake SB (2007) Extraction, purification and analysis of histones. Nature protocols
741 2:1445-1457.
742 Smolle M, Venkatesh S (2014) Transcription Through Chromatin. In: Fundamentals of Chromatin (Workman, J. L. and
743 Abmayr, S. M., eds), pp 427-489: Springer New York.
744 Soriano FX, Papadia S, Bell KF, Hardingham GE (2009) Role of histone acetylation in the activity-dependent regulation of
745 sulfiredoxin and sestrin 2. Epigenetics 4:152-158.
746 Suganuma T, Workman JL (2010) Features of the PHF8/KIAA1718 histone demethylase. Cell research 20:861-862.
747 Tea JS, Luo L (2011) The chromatin remodeling factor Bap55 functions through the TIP60 complex to regulate olfactory
748 projection neuron dendrite targeting. Neural Dev 6:5.
749 Tsankova NM, Kumar A, Nestler EJ (2004) Histone modifications at gene promoter regions in rat hippocampus after
750 acute and chronic electroconvulsive seizures. J Neurosci 24:5603-5610.
751 Tycon MA, Daddysman MK, Fecko CJ (2014) RNA Polymerase II Subunits Exhibit a Broad Distribution of Macromolecular
752 Assembly States in the Interchromatin Space of Cell Nuclei. The journal of physical chemistry B 118:423-433.
753 Tzingounis AV, Nicoll RA (2006) Arc/Arg3.1: linking gene expression to synaptic plasticity and memory. Neuron 52:403-
754 407.
755 Van de Ven TJ, VanDongen HM, VanDongen AM (2005) The nonkinase phorbol ester receptor α 1-chimerin binds the
756 NMDA receptor NR2A subunit and regulates dendritic spine density. The Journal of neuroscience 25:9488-9496.
757 Vermeulen M, Eberl HC, Matarese F, Marks H, Denissov S, Butter F, Lee KK, Olsen JV, Hyman AA, Stunnenberg HG, Mann
758 M (2010) Quantitative interaction proteomics and genome-wide profiling of epigenetic histone marks and their
759 readers. Cell 142:967-980.
760 Vogel-Ciernia A, Wood MA (2013) Neuron-specific chromatin remodeling: A missing link in epigenetic mechanisms
761 underlying synaptic plasticity, memory, and intellectual disability disorders. Neuropharmacology.
762 Wang Z, Zang C, Cui K, Schones DE, Barski A, Peng W, Zhao K (2009) Genome-wide mapping of HATs and HDACs reveals
763 distinct functions in active and inactive genes. Cell 138:1019-1031.
764 West AE, Greenberg ME (2011) Neuronal activity-regulated gene transcription in synapse development and cognitive
765 function. Cold Spring Harbor perspectives in biology 3.
766 Winter S, Simboeck E, Fischle W, Zupkovitz G, Dohnal I, Mechtler K, Ammerer G, Seiser C (2008) 14-3-3 proteins
767 recognize a histone code at histone H3 and are required for transcriptional activation. The EMBO journal 27:88-
768 99.

769 Wittmann M, Queisser G, Eder A, Wiegert JS, Bengtson CP, Hellwig A, Wittum G, Bading H (2009) Synaptic activity
770 induces dramatic changes in the geometry of the cell nucleus: interplay between nuclear structure, histone H3
771 phosphorylation, and nuclear calcium signaling. J Neurosci 29:14687-14700.
772 Xu S, Wilf R, Menon T, Panikker P, Sarthi J, Elefant F (2014) Epigenetic Control of Learning and Memory in Drosophila by
773 Tip60 HAT Action. Genetics.
774 Yu L, Wang Y, Huang S, Wang J, Deng Z, Zhang Q, Wu W, Zhang X, Liu Z, Gong W, Chen Z (2010) Structural insights into a
775 novel histone demethylase PHF8. Cell research 20:166-173.
776 Zhang K, Siino JS, Jones PR, Yau PM, Bradbury EM (2004) A mass spectrometric "Western blot" to evaluate the
777 correlations between histone methylation and histone acetylation. Proteomics 4:3765-3775.
778 Zhu Z, Wang Y, Li X, Wang Y, Xu L, Wang X, Sun T, Dong X, Chen L, Mao H, Yu Y, Li J, Chen PA, Chen CD (2010) PHF8 is a
779 histone H3K9me2 demethylase regulating rRNA synthesis. Cell research 20:794-801.
780 Zippo A, Serafini R, Rocchigiani M, Pennacchini S, Krepelova A, Oliviero S (2009) Histone crosstalk between H3S10ph and
781 H4K16ac generates a histone code that mediates transcription elongation. Cell 138:1122-1136.
782 Zlatanova J, Leuba SH (2004) Chromatin Structure and Dynamics: State-of-the-art: Elsevier.

783

784

785

Legends

Figure 1. PHF8 and TIP60 colocalize and recruit each other in neuronal interchromatin space.

A. Endogenous PHF8 immunostained with anti-PHF8 antibody (ab36068, Abcam) forms hundreds of discrete puncta that specifically localize to the interchromatin space in hippocampal neurons (representative z-slice of a hippocampal neuronal nucleus – left panel = widefield [WF], right panel = Structured Illumination Microscopy [SIM]). Scale bar corresponds to 1um.

B. Endogenous TIP60 forms puncta of roughly the same caliber as those of PHF8 above (left panel = hippocampal nucleus in WF, right panel = SIM) which also localize to the interchromatin space. Scale bar = 1um.

C. A representative field of hippocampal neurons stained with an antibody against the phosphorylated CTD of RNA Polymerase II (YSPTSPS phospho S5, abbreviated to S5P), showing that S5P, a marker of the transcription initiation complex, localizes to the same nuclear compartment as PHF8 in the nucleus. Scale bar = 1um.

D, A hippocampal neuronal nucleus outlined in blue, showing the localization of spectrally distinct PHF8-tdTomato and TIP60-CFP pseudo-colored in green and red, respectively, which overlapped completely in the nuclear interchromatin space (Merge channel, yellow pixels indicate co-localization). DAPI was used to stain the DNA (blue). Scale bar = 0.2um.

E. When TIP60 is overexpressed by itself in hippocampal neurons (middle panel, in red), endogenous PHF8 (left panel, in green) is seen to be recruited to the TIP60 puncta in hippocampal neurons (right panel, Merge). DAPI was used to stain the DNA (blue). Scale bar = 0.2um. Asterisk (*) indicates endogenous protein staining.

F. When PHF8 is overexpressed by itself (left panel, in green) in hippocampal neurons, endogenous TIP60 (middle panel) is seen to be recruited to the PHF8 puncta (right panel, Merge). DAPI was used to stain the DNA (blue). Scale bar = 0.2um. Asterisk (*) indicates endogenous protein staining.

G. Endogenous TIP60 is located within 30nm of PHF8 as shown by P-LISA, showing distinct areas where PHF8 interacts with endogenous TIP60 (red spots) on the border with DAPI-dense regions (blue). Scale bar = 0.5um.

H. Two Hek293 nuclei are shown, one is positive for PHF8 shRNA (outlined in red) while the other is not (outlined in green). Positive PHF8-TIP60 interaction hotspots were stained as red punctae. Scale bar = 0.5um.

I. Quantification of the number of hotspots found in cells transfected with PHF8, PHF8 shRNA, the mutant PHF8 F279S, or in F279S-transfected cells expressing PHF8 shRNA were quantified using Blobfinder, and the means and standard errors were displayed in a bar chart (triple asterisks indicating statistical significance using the unpaired t-test; p-value=<0.0001).

J. Double immunofluorescence confirming the existence of PHF8 in the identified PLA hotspots where PHF8 and TIP60 interact. Scale bar = 0.5um.

Figure 2. PHF8 and TIP60 physically associate to form a dual function chromatin-modifying complex

A. Coimmunoprecipitation of PHF8 and TIP60 in HEK293T nuclear extracts, where TIP60-YFP was pulled down with anti-GFP antibody and PHF8-FLAG was detected with anti-FLAG by Western blotting.

B. Pulldown of PHF8-YFP showed that TIP60-FLAG was detected in the IP fraction but not in the YFP-only control lane.

C. Endogenous coimmunoprecipitation of PHF8 and TIP60 in DIV12 cortical neuronal nuclear extracts, showing that PHF8 is able to be pulled down by both the anti-PHF8 antibody and anti-TIP60 antibody, but not the anti-GFP antibody.

D-E. Truncated constructs of TIP60 protein (A to F) containing the indicated TIP60 domains ***E.*** were fused to YFP and then co-transfected with full length PHF8-FLAG and immunoprecipitated with an anti-GFP antibody. Western analysis was performed to detect PHF8-FLAG in the immunoprecipitates using the anti-FLAG antibody. A negative control of YFP only is denoted by (-) whereas full-length TIP60 served as a positive control (+).

F-G. Total histones from HEK293 cells overexpressing PHF8, TIP60, or both PHF8 and TIP60 were separated on Triton X-Acetic Acid-Urea (TAU) gels (**F**) or conventional SDS-PAGE (**G**). Overexpression of TIP60 alone increases H3K9 acetylation in HEK293 cells for both the H3.1 and H3.3 isoforms, whereas acetylation of the non-TIP60 substrate H2BK5 was not affected. Co-expression of PHF8 and TIP60 increases H3.3 K9 acetylation to even higher levels.

H. Chromatin immunoprecipitation using an antibody specific to H3K9me2, showing that overexpression of wild-type PHF8 but not the clinical mutant F279S (legend: U=unbound or input levels of H3K9me2, B=bound or immunoprecipitated H3K9me2).

I-J. ChIP assays of HEK293T cells transfected with PHF8, TIP60, or both analyzing histone tails positive for H3K4me3, the transcriptionally-activating histone mark that is known to be bound by PHF8, show that the increase in H3K9ac (**I**) and H3K14ac (**J**) is specific to histones carrying H3K4me3, and that this histone population was enriched in H3.3 (as shown by the more intense staining of this isoform on the TAU gel; asterisk). Western blot of the same lysates using an H3.3 antibody serves as loading control. The right panel shows bar graphs quantifying the increase in H3.3K9 and H3.3K14 acetylation, relative to the untransfected control (n=3; p-value = 0.19 for PHF8 only, 0.04 for TIP60 only, 0.02 for PHF8+TIP60).

Figure 3. PHF8 removes the repressive histone mark H3K9me2 and associates with the activating histone mark H3K9ac

A. A representative hippocampal neuronal nucleus outlined in blue, transfected with PHF8-CFP (pseudo-colored green), showing a marked decrease in the repressive chromatin mark H3K9me2 (pseudo-colored blue) in the nuclear domains occupied by PHF8, which is not seen when the neuron is untransfected ***B.*** or when the mutant PHF8-F279S was transfected ***C.***.

D. The same hippocampal nucleus depicted in ***A.*** showing the association of PHF8 puncta with the histone acetylation mark H3K9ac (arrows numbered 1-6 point to regions that correspond to insets 1-6 on the right; green+red = yellow)

E. Quantitation of the intensity of H3K9me2 staining in each nucleus (each symbol marks the H3K9me2 density of a single neuron), showing that PHF8-expressing neurons have significantly lower H3K9me2 density, whereas mutant PHF8 F279S-transfected neurons show the opposite effect (*** = p-value <0.0001; ns = not significant)

Figure 4. Neuronal activity reorganizes PHF8 and TIP60 in the nucleus and effectuate histone methylation and acetylation changes

A. A representative image of a pair of hippocampal neuronal nuclei during the first 5 minutes of 4AP+Bic+Fors treatment and then at 45 minutes, showing the activity-dependent increase of PHF8 and TIP60 protein in the nucleus.

B. Neural network activity visualized by Ca^{2+} imaging (gCamp6 intensity over time), with each different-colored line representing individual neurons, before (left panel) and after (right panel) treatment with 4-AP+Bic.

C. Dot plot of nuclear levels of PHF8 and TIP60 (unpaired t-test; p-value=<0.0001; one-way ANOVA F=33.23, R^2=0.3693). Each symbol represents the intensity of PHF8 or TIP60 staining from a single neuronal nucleus, lines correspond to the mean and SEM of all neurons imaged at the indicated time points.

D. mRNA levels of PHF8 show a biphasic peak with time of chemLTP, whereas TIP60 shows an initial upregulation but a return to baseline within 45 minutes of sustained activity.

E. Time-courses of chromatin modification of neurons imaged using high-content screening (n=500-1000/site, 6 sites/well, 96-well; ImageXpress Micro, Molecular Devices) show an activity-dependent decrease in the overall per-nucleus intensity of H3K9me2 staining in neural networks treated with chemLTP, which coincides with a robust increase in H3K9acS10P.

F. Graphs of nuclear PHF8 as a function of nuclear TIP60 levels at 0, 5, 45 minutes of neural network activation in ARC-positive vs ARC-negative neurons, showing two identifiable distinct populations of neurons. The bar graph indicates levels of TIP60 (red) and PHF8 (green) as a function of time of synaptic activation (in minutes; y-axis). PHF8 and TIP60 are both highly induced within as early as 5 minutes of synaptic activation (p-value = 0.00001)

Figure 5. PHF8 and TIP60 modulate neuronal activity-induced histone acetylation at H3K9acS10P and activation of the Arc gene

A. Representative microscopic field of hippocampal neurons after 1 hour of network activation by chemLTP, showing a positive correlation between the expression of Arc (red) and Tip60 (blue) with the phosphoacetylation mark H3K9acS10P (green). The bottom panels show three different neurons that induced varying amounts of ARC protein. The neuron expressing the highest amount of ARC (3) also has high amounts of H3K9acS10P.

B. Quantification of twenty immunofluorescence-analyzed fields exemplified in ***A.*** showing a statistically significant increase in H3K9acS10P as well as endogenous TIP60 in ARC-expressing neurons (n=347 neurons; p-value = 0.00001).

C. Fusion constructs of PHF8 and its mutant F279S were individually expressed in hippocampal neurons and the next day the neuronal network was activated using ChemLTP (4AP+Bicuculline+Forskolin). After 1 hour of upregulated synaptic activity, the expression of PHF8, but not its mutant F279S, significantly increases histone acetylation at H3K9acS10P (n=397 neurons; p-value = 0.00001).

D. A representative microscopic field of neuronal nuclei after 1 hour of ChemLTP, with neuronal nuclei stained by DAPI outlined in magenta, showing the induction of ARC protein expression in a small subset of neurons, one of which had been transfected with PHF8-CFP (blue), and is high in H3K9acS10P (green).

E. A representative z-plane of a 3-D SIM image of a neuronal nucleus after 1 hour of chemLTP treatment, showing endogenous nuclear PHF8 puncta (green) and endogenous TIP60 (red) associating with the histone acetylation mark H3K9acS10P (blue). Triangles mark three selected regions, which are shown at higher magnification in the bottom panels, showing strong association between the PHF8-TIP60 complex and H3K9acS10P in the activated neuronal nucleus.

Figure 6. Knockdown of PHF8 impairs activity-dependent induction of H3K9acS10P and Arc and Fos expression

A. Neurons transfected with PHF8 shRNA1 and subsequently treated with chemLTP activation for 3 hours (DAPI-stained nuclei are outlined in magenta) were immunostained for H3K9acS10P and ARC. The right panel shows a corresponding quantification of the staining density (intensity / area / nucleus) normalized to the mean density for each condition, showing a significant decrease in H3K9acS10P induction as well as Arc gene expression (p-value = 0.0052).

B-C. Representative microscopic fields showing neurons transfected with PHF8 shRNA1 ***B.*** and PHF8 shRNA2 ***C.*** and subsequently treated with chemLTP activation for 3 hours (DAPI-stained nuclei are outlined in magenta), immunostained for products of immediate-early genes *Arc* and *Fos*. The right panel shows a corresponding quantification of the staining density (intensity / area / nucleus) normalized to the mean density for each condition, showing that shRNA knockdown by two individual PHF8 shRNAs succesfully inhibited *Arc* and *Fos* induction (b: p-values = 0.0301, 0.0408; c: p-values = 0.0002, 0.0452).

Figure 7. PHF8 and TIP60 are actively recruited to specific neuronal gene promoters

A. Recruitment of of PHF8 (red trace), TIP60 (green trace) to the transcriptional start site of the immediate-early gene Arc within minutes of synaptic activation (x-axis: time of increased network activity, in minutes). The blue trace shows H3K9acS10P enrichment at the Arc TSS after 10 minutes of synaptic activation.

B-C. Time-course ChIP followed by qRT-PCR using primers against the transcriptional start site regions of the Arc gene, Arc Synaptic Response Element, Ribosomal Protein L19 (Rpl19), Neuronal PAS Domain Protein 4 (Npas4), and Synaptophysin. Both TIP60 ***B.*** and PHF8 ***C.*** are recruited to the Arc TSS within minutes of chemLTP activation of the neural network, but not to the Rpl19, Npas4, or Synaptophysin transcriptional start sites.

Figure 8. Common interacting partners between PHF8 and TIP60 function primarily in transcription and mRNA processing

Top. A Venn diagram showing several interacting partners of PHF8 and TIP60 as identified by immunoprecipitation followed by mass spectrometry. The overlapped region in the middle represents common partners that interact with PHF8 and TIP60, which include the splicing factor SFPQ (PSF) and its partner NONO, as well as several ATP-dependent RNA helicases, and the histone chaperone Nucleolin. Proteins that have known acetylation sites are marked by a triangle (Chowdhary et al, 2009). Arrows indicate known functional interactions between identified proteins. Font size indicates the percentage of the total protein that the identified MS/MS peptides covered (large font: >25% coverage, medium font: 5-25% coverage, small font: <5% coverage). Histone proteins identified in the IP-MS are in bold face.

Bottom. A listing of the top 8 biological functions attributed to the proteins identified in the IP-MS of both PHF8 and TIP60 in order of abundance, as computed by the software DAVID (http://david.abcc.ncifcrf.gov/home.jsp) with the associated p-value and Benjamini factor, showing that interactors of PHF8 and TIP60 are enriched in the functions of RNA processing, RNA splicing, and mRNA processing.

Figure 9. Endogenous TIP60 is located within 30nm of PHF8 in the activated hippocampal neuronal nucleus

A. A maximum intensity projection of a dual color 3-D STORM image of a hippocampal neuronal nucleus that has undergone 1 hour of chemLTP. The neuron has been labeled for endogenous TIP60 (red) and endogenous PHF8 (green), showing that the two molecules closely interact in various localized puncta in the nucleus. Scale bar corresponds to 1um. The insets on the right six representative complexes at higher magnification (scale bar = 50nm).

B. A highly magnified view of two endogenous PHF8-TIP60 complexes shown in the outlined area in ***A.***. The insets on the right show 3 projections of the single-molecule interaction between PHF8 and TIP60 viewing down the X-, Y-, and Z-axis, demonstrating that the complexes formed between these two chromatin-modifying enzymes have well-defined spatial relationship. Each dot corresponds to the localization of a single molecule, and each scale bar corresponds to 50nm.

Figure 10. PHF8 and TIP60 form a tripartite complex with the splicing factor PSF and associates with newly transcribed nascent RNA

A. A maximum intensity projection of a 3-D STORM image of an activated hippocampal neuronal nucleus. Single-molecule imaging of endogenous PHF8 (green), endogenous TIP60 (red), and PTB-associated Splicing Factor (blue), with the corresponding single channel views. Each dot corresponds to the localization of a single molecule. Scale bar = 500nm.

B-C. Four representative higher magnification views of the neuronal nucleus depicted in ***A.***, showing that PSF (blue) forms a tailing structure within the interface between PHF8 (green) and TIP60 (red) viewed axially ***B.*** or longitudinally ***C.*** as a recognizable tri-partite complex. Scale bar = 50nm

Abbreviations

Arc = Activity-Regulated Cytoskeletal-associated protein (NCBI gene ID 11838 in Mus musculus)

CFP = Cyan Fluorescent Protein

DAPI = 4',6-diamidino-2-phenylindole; marker of cellular DNA

Fos = FBJ osteosarcoma oncogene (NCBI gene ID 14281 in Mus musculus)

GFP = Green Fluorescent Protein

H3 = Histone 3

H3K9 = Histone 3 Lysine 9

H3K9ac = Histone 3 Lysine 9 acetylated

H3S10p = Histone 3 Serine 10 phosphorylated

H3K9acS10P = Histone 3 Lysine 9 acetylated Serine 10 phosphorylated

HEK293 = Human Embryonic Kidney cells 293

IEG = Immediate-Early Gene

MYST = MOZ, YBF2, SAS2, TIP60 family of acetyltransferases

nm = nanometer (1×10^{-9} m)

NONO = Non-POU Domain Containing, Octamer-Binding, heterodimerizes with PSF in mRNA transcription

Pol II = RNA Polymerase II

PSF = Polypyrimidine Tract Binding protein-associated Splicing Factor, also known as SFPQ (NCBI gene ID 71514 in Mus Musculus)

SIM = Structured Illumination Microscopy

STORM = Stochastic Optical Reconstruction Microscopy

YFP = Yellow Fluorescent Protein

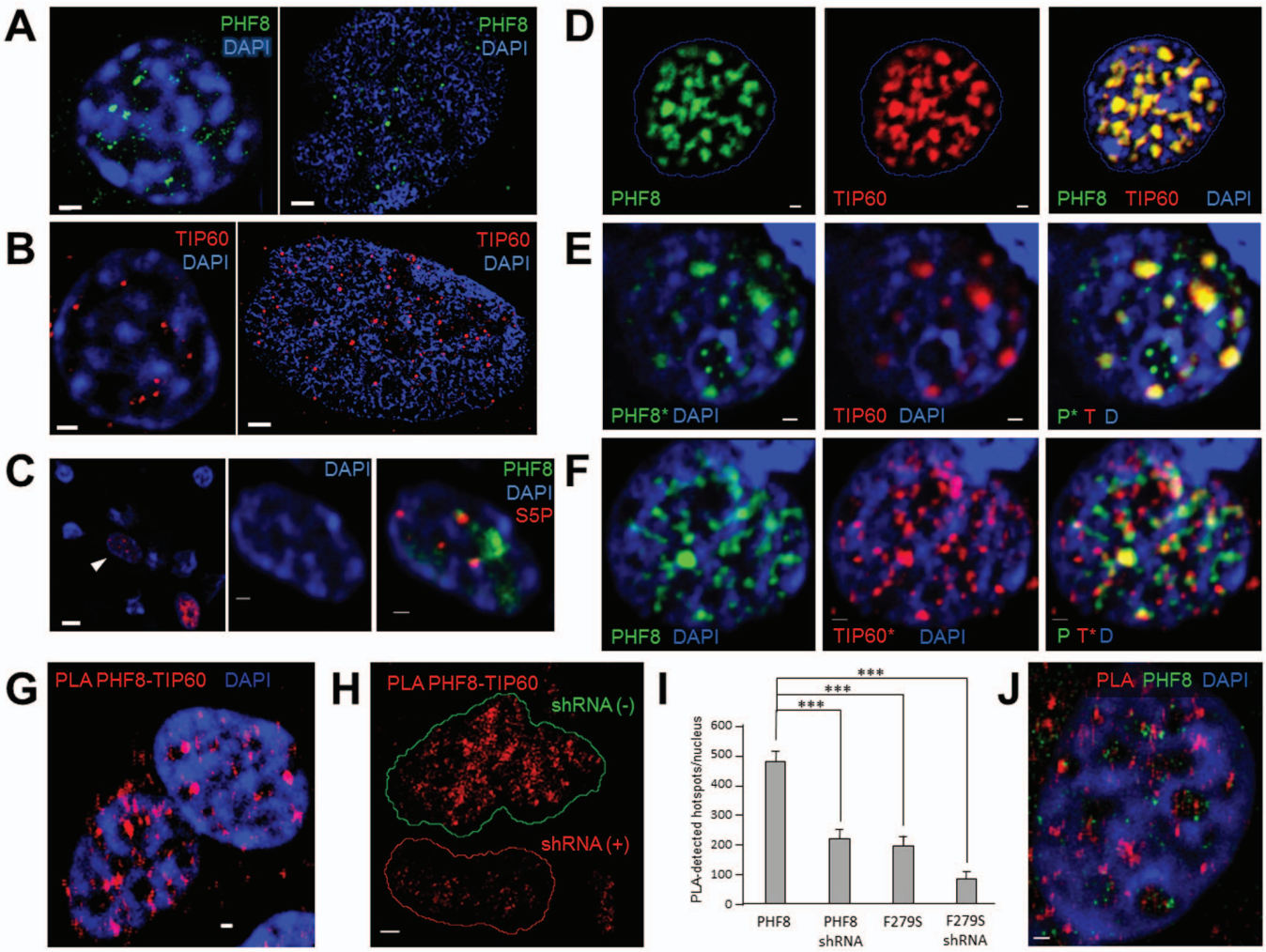

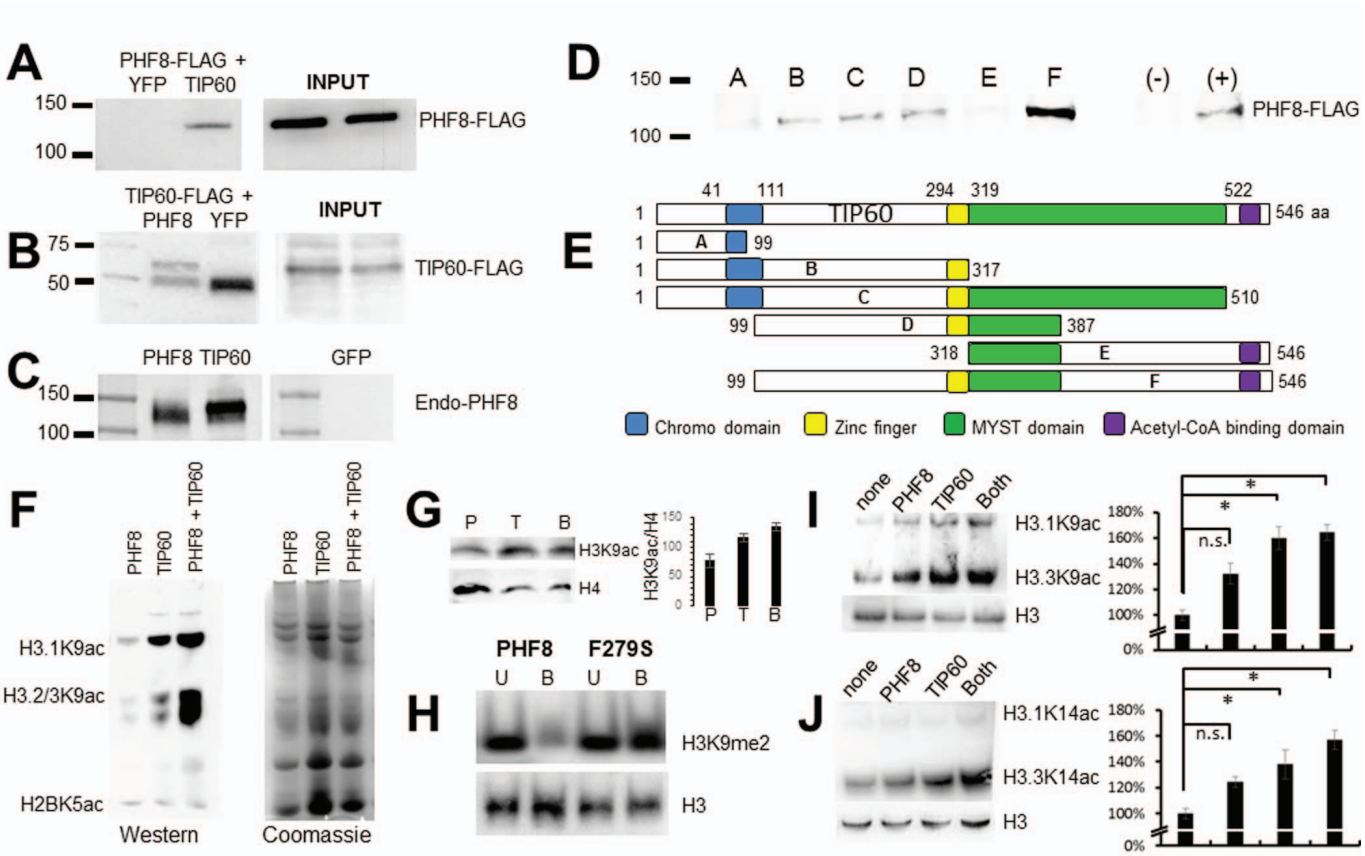

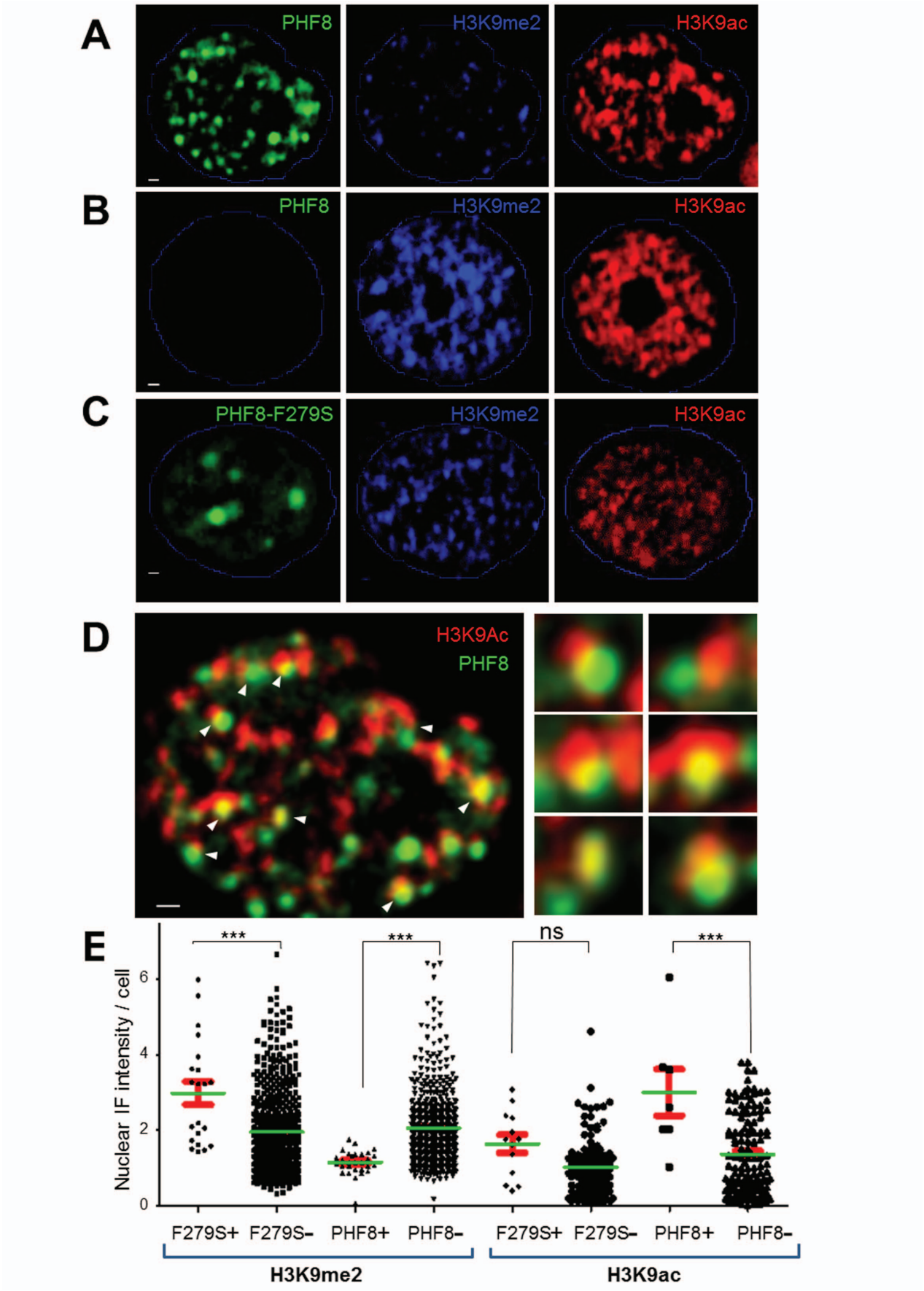

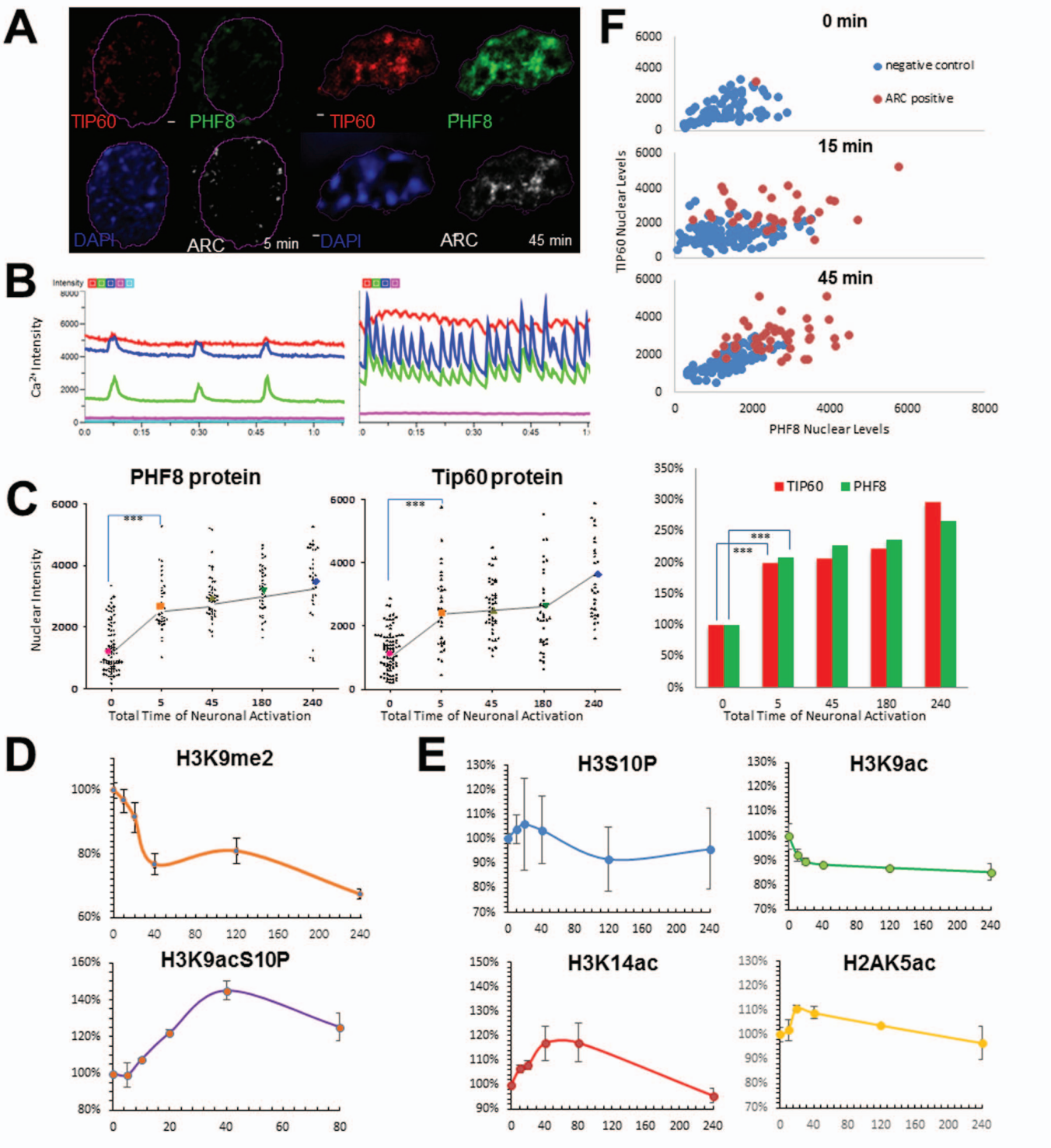

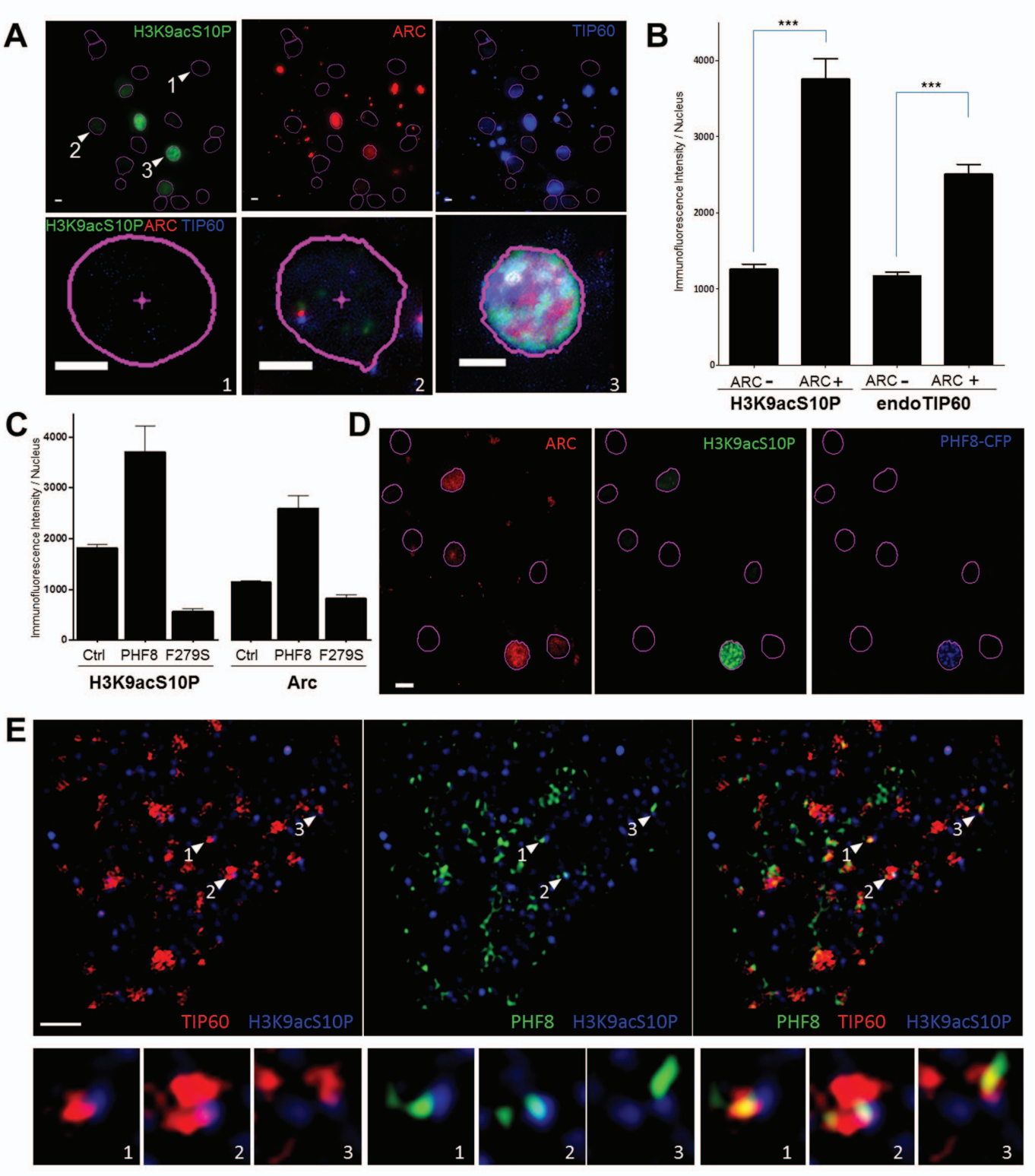

A

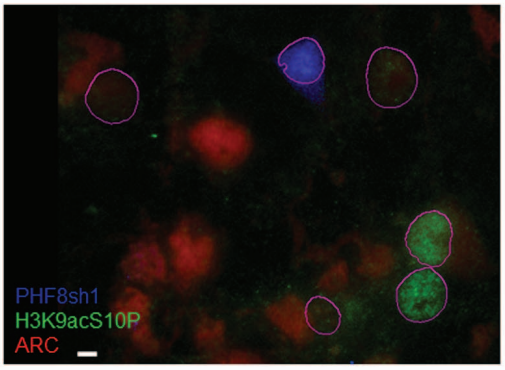

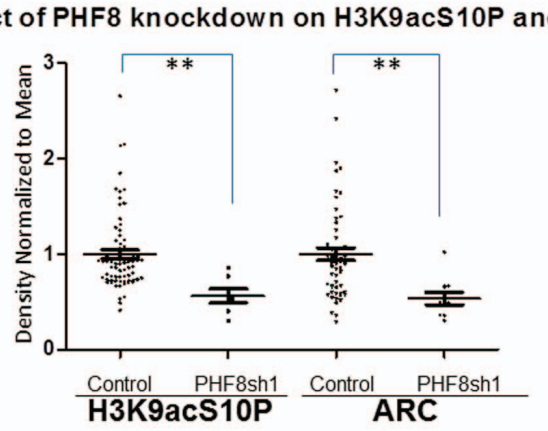

B

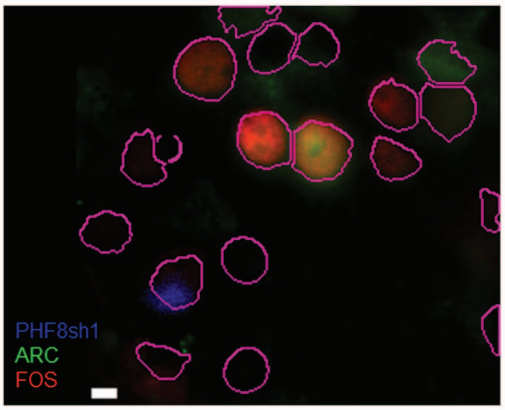

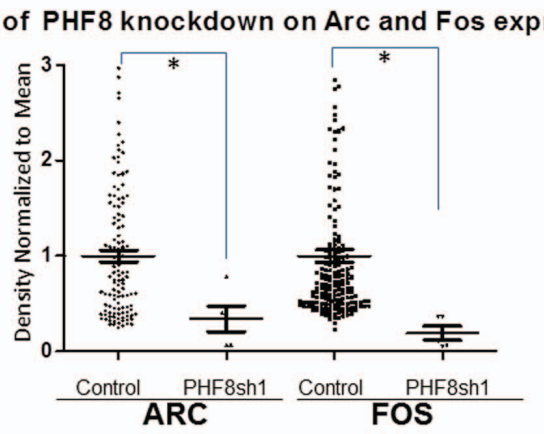

C

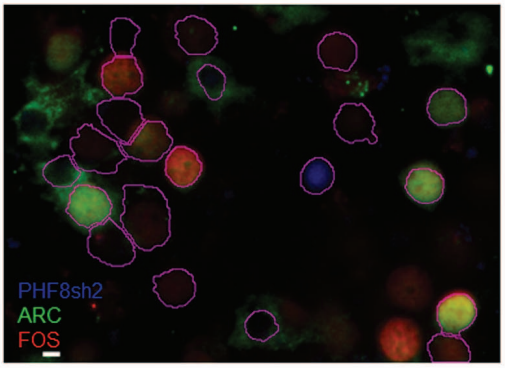

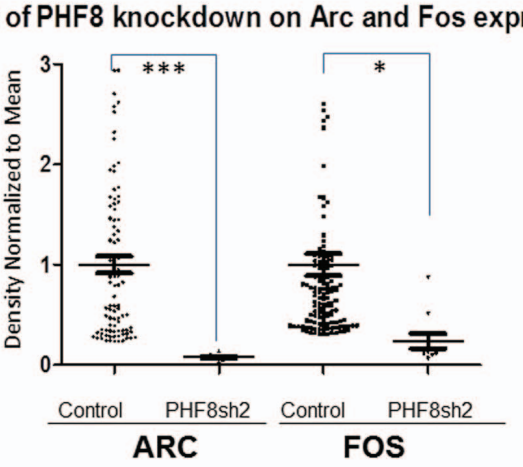

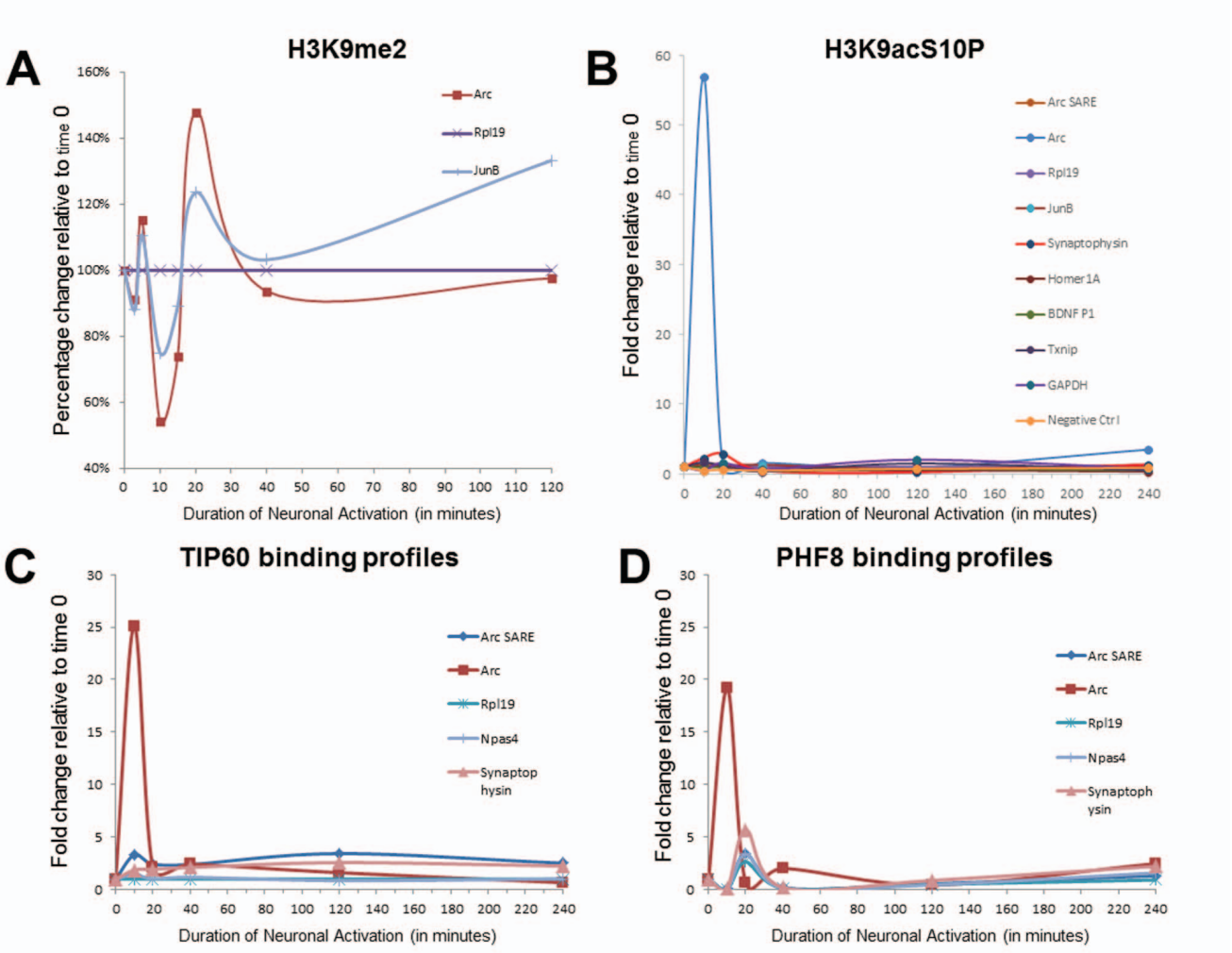

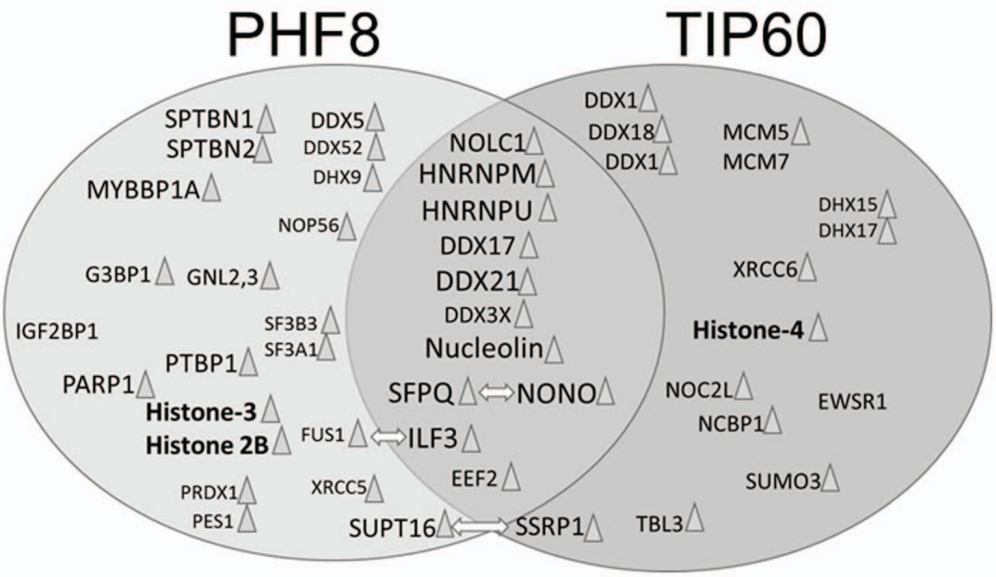

PHF8

Rank	GO Term	%	P-Value	Benjamini
1	RNA processing	23	2.1E-31	2.8E-28
2	mRNA metabolic process	19	1.1E-30	7.7E-28
3	mRNA processing	17	5.0E-28	2.3E-25
4	RNA splicing	16	6.3E-27	2.1E-24
5	nuclear mRNA splicing, via spliceosome	10	1.1E-18	3.0E-16
6	RNA splicing, via transesterification	10	1.1E-18	3.0E-16
7	DNA metabolic process	9.4	4.9E-06	3.9E-04
8	macromolecular complex assembly	9.4	3.3E-04	1.4E-02

TIP60

Rank	GO Term	%	P-Value	Benjamini
1	RNA processing	21	3.1E-06	1.4E-03
2	RNA splicing	14	6.7E-05	7.6E-03
3	mRNA processing	14	1.4E-04	1.3E-02
4	mRNA metabolic process	14	3.5E-04	2.6E-02
5	DNA metabolic process	12	9.5E-03	2.5E-01
6	response to DNA damage stimulus	11	1.1E-02	2.7E-01
7	nuclear mRNA splicing, via spliceosome	8.8	2.2E-03	1.4E-01
8	RNA splicing, via transesterification	8.8	2.2E-03	1.4E-01